Mapping and visualization of the Earth's topography and spatio-temporal change: Selected case studies of mountainous terrain

Habilitation Treatise
(Habilitationsschrift)

VIKTOR KAUFMANN

viktor.kaufmann@tugraz.at
Institute of Remote Sensing and Photogrammetry
Graz University of Technology, Austria

Abstract

The subject matter of this paper is the visible surface of the Earth, the Earth's terrain. The Earth is a dynamic system. Its surface is not static but in a constant process of change through time. Endogenous and exogenous forces as also anthropogenic impact (direct and indirect) are driving elements for land surface change. Based on selected case studies of preferably mountainous terrain carried out by the author, it is intended not only to present various observation techniques for deducing relief information and its spatio-temporal change but also to show the technological progress of topographic mapping over the last two decades. The focus is clearly on remote sensing techniques facilitating area-wide coverage. Single point based geodetic measurements have also been carried out enhancing the spectrum of observation techniques. Field work has been identified as indispensable in most of the practical work. The present case studies are inherently highly interdisciplinary. Time constraints and limited financial means sometimes required unconventional solutions, which are also considered in this publication.

The following geomorphologic landforms will be treated in this paper: *a volcanic landscape* (Chilean and Argentine Andes), *badlands* (Southern Italy), a *glacier* (Austrian Alps), *rock glaciers* (Austrian Alps), and *a landslide* (Austrian Alps). Remotely sensed data have been recorded either with space-borne, airborne, or ground-based imaging systems. This paper is primarily concerned with optical image data, however, radar data was also used where appropriate. Photogrammetric data capture on analog film is being progressively replaced by digital recording using digital sensors. Analog photogrammetric restitution apparatus was replaced by analytical stereoplotters, which in turn were finally replaced by state-of-the-art digital photogrammetric workstations. As far as digital photogrammetry is concerned, image data can be either still analog film which needs to be digitized or original digital data originating from a digital sensor, for example, a digital aerial camera. In this paper a special focus is also placed on low-priced digital SLR consumer cameras. Digital photogrammetry and modern techniques of computer vision provide new possibilities in terms of automating the image evaluation process. Bulk data can be processed, multi-ray geometry can be introduced, and stereovision capability is no longer needed. All this facilitated "democratization" of photogrammetry. The use of photogrammetric and other remote sensing techniques is no longer confined to specialists. For example, a proposal will be made on how to carry out glacier monitoring by a layperson using terrestrial "photographs" taken with a digital SLR camera.

The paper is structured according to the main landforms mapped by the author in the course of time. For detailed information the reader is referred either to the references given or to the papers included in the Appendix to this document.

Results of photogrammetric and geodetic work are presented numerically and/or graphically. Topographic and thematic maps were compiled visualizing the spatial (2D or 3D) information retrieved. The spatio-temporal evolution of certain processes of the Earth's surface is sometimes best shown by computer animation. A "glacier video" has been produced in order to visualize the course of deglaciation of two small cirque glaciers located in the Austrian Alps. Small surface movements, for example of a rock glacier, can be revealed using co-registered multi-temporal image data. Surface flow/creep velocity can be retrieved from these data. Computer animations can help to visualize surface change for easy recognition by the human observer. The present publication comprises several printed maps and a CD-ROM showing the "glacier video", as also other computer animations elaborated by the author.

Keywords: Remote sensing, photogrammetry, cartography, topographic mapping, visualization, change detection, badlands, volcano, glacier, rock glacier, landslide, monitoring, Basilicata, Chile/Argentina, Austrian Alps.

1. Introduction

A number of definitions need to be given at the start for purposes of clarification. The International Society for Photogrammetry and Remote Sensing makes no explicit distinction between *photogrammetry* and *remote sensing,* stating that "Photogrammetry and Remote Sensing is the art, science, and technology of obtaining reliable information from non-contact imaging and other sensor systems about the Earth and its environment, and other physical objects and processes through recording, measuring, analyzing and representation (ISPRS, 2009)." From a historical point of view, "Photogrammetry" (cp. Albertz, 2007) is by far the older term (1867), whereas "Remote Sensing" was not introduced until 1960. Photogrammetry and remote sensing are converging more and more due to progress in sensor and computer technology. Without giving any more detailed definition of photogrammetry, which was originally concerned primarily with the geometric reconstruction of three-dimensional (3D) objects such as cultural heritage buildings, the Earth's surface, etc. based on central perspective images (photographs of pinhole-type cameras), the author proposes to see photogrammetry as an integral part of remote sensing (cp. Konecny and Lehmann, 1984, p. 11). *Computer vision* is a prospective field of computer science. Its principal idea is to emulate the human vision system on computer hardware, which also includes automatic 3D object reconstruction based on digital images. In the meantime photogrammetrists have adopted algorithms of the computer vision world, and the term *photogrammetric computer vision* was born (Leberl, 2001).

The following definitions have been taken directly from Wikipedia (Wikipedia, 2009) and provide the basis for a common understanding. We keep them short and simple. *Topography* is the study of the Earth's surface features and is concerned with local detail in general, including not only relief but also vegetation and human-made features, and even local history and culture. "Topography" is sometimes used synonymously with relief. A *Topographic map* is a detailed and accurate graphic representation of cultural and natural features on the ground. Topography specifically involves the recording of *relief* or *terrain*, the three-dimensional quality of the *land surface*, and the identification of specific landforms. *Geomorphometry* is the science of quantitative land surface analysis (cp. also Hengl and Reuter, 2009). Terrain, or relief, is the third or vertical dimension of land surface. A *digital elevation model (DEM)* – also sometimes called a *digital terrain model (DTM)* – generally refers to a representation of the Earth's surface (or subset of this), excluding features such as vegetation, buildings, bridges, etc. A *digital surface model (DSM)* on the other hand includes buildings, vegetation, and roads, as well as natural terrain features. The DEM provides a so-called bare-earth model, devoid of landscape features. A DEM can be represented as a raster or as a triangulated irregular network. *Geomorphology* is the study of landforms and the processes that shape them.

Kääb (2005) and Chandler et al. (2007) are two recent references providing state-of-the-art information on earth surface mapping and change detection using aerial photographs and satellite image data.

This paper summarizes the work carried out by the author as a principal investigator at different test sites located in South America and Europe. Chapter 2 reports on an unconventional mapping project accomplished in the Andes of South America, dealing with a volcanic landscape. The badlands of the Basilicata region in Southern Italy were the subject of detailed relief mapping and change detection as described in Chapter 3. The remaining Chapters 4 to 10 are devoted to Austrian test sites. Chapter 4 deals with two adjacent small cirque glaciers, Gössnitzkees and Hornkees, located in the Austrian Alps. The main focus is on the documentation of glacier retreat due to atmospheric warming, which also has an impact on the periglacial environment to which rock glaciers belong by definition. Monitoring projects running at five different rock glaciers, i.e., Outer and Inner Hochebenkar rock glaciers (Ötztal Alps), Doesen rock glacier, Hinteres Langtalkar rock glacier, and Weissenkar rock glacier (all Hohe Tauern Range) will be introduced to the reader in Chapters 5 to 9. The last case study to be presented in this paper is devoted to a landslide prone area near Krimml, Salzburg, which is outlined in Chapter 10. This overview paper concludes with acknowledgments.

The author's homepage (Kaufmann, 2009) provides online access to photographs, written documents, and other collateral data associated with the case studies presented in this paper.

2. Volcano Nevado Ojos del Salado (Chile, Argentina)

2.1. Location and geographical setting

Nevado Ojos del Salado (27°10' S, 68°30' W; see Figure 1) is the second highest mountain of both Americas and the world's highest active volcano. It is located in a remote area in the High Cordillera of the Andes at the Chilean-Argentine border east of Copiapó. There are no records of historic volcanic eruptions. The current volcanic activity is restricted to persistent fumaroles in the summit area (González-Ferrán, 1995; de Silva and

Francis, 1991). The height of the volcano has been a matter of repeated measurements and also debates over the past few decades (Kaufmann, 1998a; Remark: References with the name of the first author underlined are attached to this publication in full length). The official Chilean topographic maps give an elevation of 6,880 m for the summit. According to Buchroithner (2006), the Instituto Geográfico Militar (IGM) at Santiago de Chile has determined a new, more precise height of the peak of Nevado Ojos del Salado using GPS measurements, resulting in an altitude of 6893 m above mean sea level. For more details on the geographical setting of Nevado Ojos del Salado and its surroundings, the interested reader is referred to Sulzer (1994) and Gspurning et al. (2006).

Only little information was available on this remote and deserted area at the time of investigation (1994) due to political reasons – the borderline between Chile and Argentina runs through the Ojos del Salado volcanic unit. Wolfgang Sulzer, geomorphologist at the Institute of Geography and Regional Science, University of Graz, was especially interested in the volcanic geomorphology of this area and had been examining recent glaciation of Nevado Ojos del Salado and the other volcanic cones and mountain ridges in the surroundings. Interest in this area was not restricted to science, however, since it had also developed into a significant attraction for mountaineering, as Nevado Ojos del Salado started to become a more and more fashionable target for climbers at that time. Both the scientist and the climbers were therefore in urgent need of up-to-date topographic maps at reasonably large scales.

Figure 1. Terrestrial view of Nevado Ojos del Salado (6893 m) seen from westerly direction. Photograph taken by V. Kaufmann on 17 November 1994 during a four-day field excursion from Copiapó, III Región de Atacama, Chile, to the Chilean-Argentine border area of Paso de San Francisco (4747 m).

2.2. Definition of task

Topographic information (relief, drainage pattern, surface texture, etc.) was needed as a basis for geomorphological mapping. It was not possible to order topographic maps from the Argentine mapping authorities. Only Chilean topographic maps at 1:500,000 and 1:250,000 covering the area of interest were at our disposal. It was planned to update the content of these maps using both low-priced satellite image data and official aerial photographs. The project involved the production of a detailed topographic map of the area of interest at 1:15,000 scale and the generation of a high-resolution digital elevation model (DEM), orthophotos and stereo-orthophotos from the primary data.

The evaluation of both the space-borne and airborne photographs is described in detail in Kaufmann (1998a). Most of the practical work was done by the author's former student Robert Benzinger (Benzinger, 1994).

2.3. Topographic mapping using aerial photographs and space shuttle earth observation photographs

Five panchromatic aerial photographs at 1:30,000 scale dating from 1961 were provided by Heinz Badura of Schladming, Austria, as black-and-white paper prints. He had acquired these photographs from IGM, Santiago de Chile, during an earlier visit to Chile. Since the existing small scale topographic maps could not be used to retrieve ground control points (GCPs) for proper photogrammetric absolute orientation of the triangulated airborne stereomodels, a rather unconventional solution was pursued to solve this scale-dependent problem.

Earth-looking photographs of the Space Shuttle Earth Observations Project (SSEOP) were ordered as color transparencies (cp. Figure 2) from the Earth Data Analysis Center at the University of New Mexico.

The current NASA-Johnson Space Center database of "Astronaut Photography of Earth" holds some 780,000 frames (analog photographs and digital images) dating back to the early 1960s. Approximately 330,000 images of the database were taken by astronauts of the International Space Station (ISS) using various high-resolution consumer-grade digital cameras. More information on flight missions and photograph/image browsing can be obtained from "The Gateway to Astronaut Photography of Earth" (NASA-JSC, 2009). In this context it is worth mentioning that historical earth observation data, also from American spy satellites are now readily available to the public. In 1996 the author bought a high-resolution CORONA stereopair (year of acquisition 1969) covering the area of interest. Please see the stereogram in (Kaufmann and Sulzer, 1997, p. 171).

Photogrammetric orientation of a single SSEOP stereomodel and subsequent feature extraction was done using an analytical DSR-1 stereoplotter of Kern and CRISP software (Fuchs and Leberl, 1984). In contrast, the aerial photographs were triangulated using a Zeiss-Jena Topocart stereoplotter, which had been upgraded from analog to analytical (Adams Technology, Australia), and PATM-386 software (block adjustment with independent models, H. Klein/F. Ackermann, 1988). Ground control points for absolute orientation of the aerial photographs were taken from the SSEOP stereopair. Identification of common natural points was quite troublesome, since the Topocart stereomodels were reversed from left to right. The accuracy obtained was ±180 m in planimetry and ±45 m in height according to the coordinate system defined by the Shuttle stereopair. Subsequently, detailed photogrammetric feature extraction was performed. A DEM of the Nevado Ojos del Salado volcanic complex was computed with a grid spacing of 10 m. As a result, a combined image-line map at 1:15,000 scale was produced. The digital orthophoto produced has a ground sampling distance (GSD) of 2.5 m. A stereomate was generated for easier 3D vision. The topographic data available served as a good basis for the anticipated morphological study (see geomorphological interpretation compiled by Sulzer, 1994).

Figure 2. SSEOP STS61C-45-20 color photograph acquired on 13 January 1986. Image data provided by the Earth Data Analysis Center, University of New Mexico. Image scale of the original photograph is approximately 1:840,000.

2.4. ERS-1 radar images

Two same-side ERS-1 Synthetic Aperture Radar (SAR) stereopairs covering the area of interest were provided free of charge by the European Space Agency (ESA). The ERS-1 SAR Precision Images have a pixel spacing of 12.5 m. SAR inherent speckle noise was reduced by means of block averaging in order to improve the visual perception of the image content. An ERS-1 SAR stereogram is shown in Kaufmann (1998a). A procedure for georeferencing these SAR scenes by means of stereo-radargrammetric methods is outlined in Chapter 3.

2.5. Map "Nevado Ojos del Salado 1:100,000"

In 2004 the German Alpine Club published the map "Nevado Ojos del Salado" at 1:100,000 scale. This map had been prepared at the Institute of Cartography, Dresden University of Technology, under the project management of Manfred Buchroithner (Buchroithner, 2006; Fleischer, 1996). For better depiction of the central part of the volcano Nevado Ojos del Salado, an inset map at 1:35,000 scale was produced based on the high-resolution DEM obtained in the present study. The respective section of the map is shown in Appendix A3 (AV-Map, 2004).

2.6. Acknowledgments

The software for feature extraction using the Zeiss-Jena Topocart stereoplotter was developed by the author's colleague Walter Klostius, Institute of Remote Sensing and Photogrammetry, Graz University of Technology. In 1994 the 1:50,000-scale map sheet of "Nevado Ojos del Salado" No. 2700-6830 was published by IGM, Santiago de Chile. The author was able to acquire the map sheet with the imprint 0001.

3. Badlands in Basilicata (Southern Italy)

3.1. Introduction

The term "badlands" was originally used to describe intensely dissected natural landscapes where vegetation is sparse or absent and which are useless for agriculture (Bryan and Yair, 1982). The formation of badlands is determined by several environmental factors of the area involved, such as geology, relief, precipitation structure, vegetation cover, and land utilization. Badlands are a common landscape in Italy, especially in the south of the country. Badland regions in Italy are underlain preferably by blue-grey Plio-Pleistocene clays (Guerricchio and Melidoro, 1982). Two main landforms with different forming processes and individual appearance are distinguished (Alexander, 1982): (1) *Calanchi* (singular: calanco). Calanchi are intensively dissected landscapes, representing rill and gully landforms and a dense dendritic drainage network. Knife-edged ridges are developed on the slopes, headwalls are often horseshoe-shaped, and sharp breaks of slope occur at the base of the calanchi slopes. (2) *Biancane* (singular: biancana). Biancane are small, conical or dome-shaped forms rising a few meters above pediment-like surfaces of low inclination. They may occur singly or in groups.

Badlands in the Mediterranean semi-arid climate, with hot dry summers and mild winters with high intensity rainfall, may develop piping gullies which results in subsurface drainage. The denudation process is enhanced by tunnel erosion (Bryan and Yair, 1982).

Badland research has intensified over the last decade. The origin of calanchi and biancane is still a matter of debate. For more details see Battaglia et al. (2002), Clarke and Rendell (2006), and Farifteh and Soeters (2006).

3.2. Location and geographical setting

The study area (40°17'N, 16°16'E, 126.5 km^2) is located in the NE part of the Sant' Arcangelo basin, which is part of the catchment area of the Agri river and belongs to the Basilicata region in Southern Italy. This area (see Geomorphological Base Map 1:50,000, Kaufmann and Lieb, 1997) covers the major part of one of the largest badland areas in Italy. Detailed morphological studies, however, were confined to a smaller area (5.625 km^2) in the center (see Geomorphological Study Map 1:10,000, Kaufmann and Lieb, 1997). The region has been the study area for students and researchers of the International Institute for Geo-Information Science and Earth Observation (ITC, Enschede, the Netherlands) for many years (Farifteh and Soeters, 2006; Verstappen, 1983). The author conducted field studies in close cooperation with ITC in the years 1990, 1991, 1992, and 1993. A concise description of the geographical setting of the area of interest is given by Kaufmann and Lieb (1997). For further details the reader is referred to Verstappen (1983), and Farifteh and Soeters (2006). Figures 3 to 5 show typical landforms of the badland environment of this area.

Figure 3. Ground view of a well-developed badland area with biancane and calanchi near Alianello in the Sant' Arcangelo basin. Viewing direction towards northeast. Photograph taken by V. Kaufmann on 5 May 1990.

Figure 4. Ground view of the badland area as seen in south-westerly direction. The gently sloping north-facing back-slopes are vegetated. In the foreground a swarm of biancane can be seen. A person is standing on top of a biancana, right in the center of the photograph. Photograph taken on 5 May 1990.

Figure 5. Piping gullies are frequent in the study area. The vertical pipe seen in the photograph is approx. 2-3 meters deep. Photograph taken on 5 May 1990.

3.3. Objectives of investigation

Three-dimensional surface information (relief, drainage pattern, land cover, etc.) is needed for geomorphometric analysis and environmental studies. Such information can be efficiently retrieved from remotely sensed data. Image data, such as a single high-resolution Russian KVR-1000 space photograph, and panchromatic SPOT-1, ERS-1 SAR, and spectrozonal KFA-1000 stereopairs were acquired for comparative studies. Aerial photographs of 1976 and 1990 were available as a means of reference. The investigations were carried out at a time when analytical stereoplotters were still used and digital photogrammetric methods (= digital image restitution) began to supersede classical photogrammetric work flow based on analog image data (=analytical restitution). The results were published in Kaufmann et al. (1994), Kaufmann and Fastner (1995), and Kaufmann and Lieb (1997).

3.4. New possibilities with high-resolution space images (KVR-1000)

In the early 1990s, high-resolution space images were gradually declassified and thus became available on the open market (Konecny, 1995 and 2004). In 1993 the author started to investigate the potential of this kind of image source for large-scale environmental studies. In particular, he was interested in surface change detection. A Russian high-resolution panoramic KVR-1000 photograph was purchased in digital format (DD-5) from the Russian "State Center Priroda" in Moscow. The photograph was taken early in the morning on 30 December 1990. Although long shadows are present in the image, the badland landforms, which are restricted more or less to the southward facing slopes, can be recognized very well.

Practical applications of KVR-1000, also named KWR-1000 (Russian: камера высокого разрешения, English: high-resolution camera) image data have mainly been reported for urban areas (e.g., Kostka and Sharov, 1993; Riess et al., 1993; K.-U. Kaufmann and Buchroithner, 1994).

The task was to prepare two KVR-1000 orthoimage-based maps at 1:50,000 scale and at 1:10,000 scale, respectively. Orthorectification of the satellite image data was accomplished using GCPs extracted from aerial photographs (1990). Helmert transformation was found to be appropriate. The geometric fidelity of the rectified satellite image was controlled by superimposition of a digital 1:5,000 geomorphological map derived from older photographs (1976). Please see both the Geomorphological Base Map 1:50,000 and the Geomorphological Study Map 1:10,000 in (Kaufmann and Lieb, 1997, Appendix A4). The practical example showed that map up-dating using KVR image data, which has a nominal ground resolution of 2 meters, is feasible, at least for sunlit areas. Relief change in the badlands, for example by bulldozing of biancane, was revealed perfectly (see the large-scale map). Map up-dating of the traffic network was also possible.

In an academic exercise, the author computed the exact acquisition time (±3 minutes) of the KVR-1000 image by means of astronomy using shadow information obtained from the orthoimage and ephemerides of the sun. The interested reader is referred to Kaufmann and Fastner (1995).

3.5. Comparative study on 3D topographic mapping using SPOT-1 and ERS-1 SAR stereopairs

With the advent of new operational satellite-based earth observation systems, such as SPOT-1 (pushbroom scanner, start in 1986) or ERS-1 (synthetic aperture radar, start in 1991), not only experimental methods but also established techniques for 3D mapping of the Earth's surface using stereoscopic image pairs were revised and further developed. The badland area of Sant' Arcangelo basin served as a test site for comparative studies on the use of panchromatic SPOT-1 Level 1B data (1986, 10 m ground resolution) and ERS-1 SAR Precision Images (1992, pixel spacing of 12.5 m) for (1) generating DEMs and (2) retrieving 3D topographical linear features, such as drainage pattern, other important morphological structures, and land use boundaries. Two different methods of stereo mapping procedures were investigated in this study:

1. the classical or hybrid method using film transparencies with an analytical stereoplotter,
2. the semi-automatic digital method using image correlation techniques.

3.5.1. Classical or hybrid method

The principal concept of this method is that an analytical stereoplotter is used for stereo restitution of original analog image data or digital-to-analog converted image data. Data capture is done interactively by a skilled operator. Software, originally developed for the evaluation of frame cameras, was adapted to handle CCD line scanner and side-looking radar geometries. A flow chart describing the main processing steps for the radargrammetric evaluation of ERS-1 SAR data using an analytical plotter is shown in Kaufmann et al. (1994, Figure 3). In our study we used an analytical stereoplotter DRS-1 of Kern with dedicated software for both space-borne line scanner imagery (Fuchs, 1986) and side-looking radar imagery (Raggam, 1984) developed at the present Institute of Digital Image Processing, Joanneum Research, Graz.

Rigorous methods for the geometric processing of SPOT-1 images have also been developed and implemented for other analytical stereoplotters, e.g., for Zeiss Planicomp by Konecny et al. (1987) and for Wild Aviolyt BC2 by Trinder et al. (1988).

Four different methods (clinometry, stereoscopy, interferometry and polarimetry) can be applied to elevation extraction from satellite SAR data (see review paper Toutin and Gray, 2000). While implementation of the stereoscopic method using an analytical plotter remained scarce (see reference given above), stereoscopy was much easier to implement in the digital domain, with or without stereo-viewing capability, including SPOT applications.

3.5.2. Semi-automatic digital method

The data flow for processing is completely digital. The image data is either born digital or digitized analog images. A flow chart describing the main processing steps for ERS-1 data is shown in Kaufmann et al. (1994, Figure 5). The processing chain is semi-automatic, since human interaction is needed for several processing steps. Geometric co-registration (epipolar resampling) is carried out to support image matching. Measurement of homologous points (mass points) for surface reconstruction is automated. RSG software of the present Institute of Digital Image Processing, Joanneum Research Graz, was used for this study.

Baltsavias and Stallmann (1994) were the first to explicitly use the SPOT geometry in matching, restricting the search space in one dimension, and simultaneously providing pixel and object coordinates. Their algorithm is based on a modified version of the Multiphoto Geometrically Constrained Matching (MPGC).

Toutin (1995) was one of the first to present a digital photogrammetric workstation (DVP system) for rigorous stereomodel set-up, automatic DEM generation and interactive 3D feature extraction for various types of stereo imagery, including SPOT-1 and ERS-1 data. Today, modern digital photogrammetric workstations (DPWs) are primarily devoted to optical data (e.g. Z/I ImageStation, see Biard et al., 2004). The operational evaluation of radar data is mostly restricted to special solutions.

3.5.3. Main findings of the comparative study

The outcome of the study was published in Kaufmann et al. (1994) and Kaufmann and Fastner (1995). The main findings are summarized in this paper.

SPOT-1
The SPOT-1 DEMs, i.e., two DEMs derived with the hybrid method for different image scales and the DEM obtained using the semi-automatic digital method, were checked using a high-resolution DEM derived from the aerial photographs of 1976. In all three cases significant height offsets in the range of +12 m to -14 m were observed. Both DEMs obtained using the hybrid method (interactive mapping) were of higher quality than the semi-automatically derived DEM. It was found that an experienced operator can better deal with local radiometric differences in the stereopair. Remark: Along-track image acquisition capability of modern space-borne pushbroom scanners, e.g., SPOT-5 HRS, avoids this specific problem of temporal decorrelation of surface reflectance (cp. Poli et al., 2004).

ERS-1 SAR
DEMs derived from stereoscopic ERS-1 SAR data showed a variable systematic shift in height against the DEM derived from SPOT-1. The standard deviations of height differences are about ±27 to ±34 m. The values obtained agree well with those obtained by others (cp. Li et al. 2006). DEMs derived from stereoscopic ERS-1 SAR do not fulfill the requirements for high precision SAR geocoding.

Hybrid method:
No stereo fusion of opposite-side stereopairs was possible. Due to relief displacement inherent in side-looking radar, the viewed stereo model is geometrically highly distorted. Proper relief impression is disrupted in foreshortening and layover areas (“floating clouds above ground”). Decorrelation of image brightness is experienced in all rather flat areas. Drainage patterns and prominent geomorphological features could be mapped to a great extent compared to SPOT. However, systematic offsets in planimetry were observed.

Semi-automated method:
The proposed image matching algorithms did not prove optimal.

3.5.4. Evaluation of the KFA-1000 stereopair

Spectrozonal KFA-1000 (Russian: космический фотографический аппарат, English: space photographic apparatus) images, i.e. Russian high resolution space photographs, are another source of earth observation data suitable for topographic mapping. Today, of course, these photographs are valuable historical documents for change detection analysis.

A KFA-1000 stereopair of 1992 was provided by the Russian "State Center Priroda". Detailed information on the photogrammetric processing (photogrammetric orientation using the analytical plotter DSR-1, orthorectification) of the image data is given in Kaufmann et al. (1994). Photogrammetric triangulation and topographic mapping using KFA-1000 photographs has been widely discussed in literature (cp. Sirkiä and Laiho, 1989; Krämer and Illhardt, 1990; Jacobsen, 1992; Csaplovics et al., 1994).

Since the frame size of the original film transparencies is 30 cm × 30 cm, working copies of 23 cm × 23 cm size covering the area of interest and including at least three fiducial marks were prepared. Relative orientation of the stereopair was done using the given asymmetrical radial lens distortion. GCPs of the study area were taken for absolute orientation. Because of the small base-to-height ratio of 0.14, topographic mapping in respect to relief was not performed on the analytical plotter. Instead, the photographs were scanned and digitally rectified using the software system GAMSAD developed by Kaufmann (1984), employing a strict photogrammetric model using the asymmetrical lens distortion given and the DEM derived from SPOT-1 data.

The author investigated not only the geometric potential of KFA-1000 photographs but also that of panchromatic KFA-3000 photographs with a focal length of 3 meters. A KFA-3000 photograph covering a test site near the city of Feldbach (46°57'N, 15°54'W, Austria) was also successfully photogrammetrically oriented and digitally rectified using GAMSAD. An orthophoto map at 1:10,000 scale was generated. Results were published in Klostius et al. (1994), which also comprises a critical analysis of the potential of Russian high-resolution satellite image data for cartographic purposes. For purposes of comparison, reference is also made to Kraus and Sindhuber (1996).

Remark: As regards topographic mapping from space, the author's first contribution towards this topic was the photogrammetric orientation and subsequent 3D data compilation of a Large Format Camera (LFC) stereopair covering the city of Kathmandu, Nepal, using an analog stereoplotter Zeiss Planimat D2. This work was supported by the author's colleague Reinfried Mansberger. For technical details see Kostka (1987). The photogrammetric manuscript obtained served as a topographic basis for map production (see map "Kathmandu Valley 1:100,000", LFC-Map, 1987, Appendix A1).

3.6. Acknowledgments

Ch. Hsu, H. Beissmann and R. Hengsberger from the former Institute of Cartography, Austrian Academy of Sciences, Vienna, were responsible for map design, digital cartography and reproduction of the two maps of the Sant' Arcangelo region. Their commitment is very much appreciated by the author. Large parts of the analysis of the ERS SAR and SPOT-1 data were carried out by former students of the author, i.e., Wolfgang Mattner and Johann Schnell, during diploma studies. Ulrike Fastner and Walter Klostius supported the GPS measurements carried out in the badlands. The author thanks Johann Raggam from the Institute of Digital Image Processing, Joanneum Research Graz, for the correct set-up of the analytical stereoplotter. The author also wishes to thank Robert Kostka from the Institute of Photogrammetry and Remote Sensing, Graz University of Technology, for providing funds (FWF Project P8048 GEO), especially for printing the maps. Russian transliteration was provided by Aleksey Sharov.

4. Gössnitzkees and Hornkees glaciers (Carinthia, Austrian Alps)

4.1. Introduction

Gössnitzkees (46°56'00"N, 12°45'45"E) and Hornkees (46°58'25"N, 12°46'40"E) are two neighboring cirque glaciers located at the head of Gössnitz valley in the Schober Mountains, Hohe Tauern Range, Austria (see Figure 6 and also the orthophoto map "Gößnitzkees- und Hornkees, Schobergruppe – Luftbildkarte 1:10 000", GLACIER-Map, 1998, Appendix A13). "Kees" is the local name for glacier. Both glaciers belong to the Carinthian part of the Hohe Tauern National Park. Glaciological research in the Schober Mountains was initiated by Lieb (1987) and Buchenauer (1990). A coherent overview of the Schober Mountains as a natural landscape is given in Lieb and Krobath (2006). The geographical setting of both glaciers is described in detail in Lieb (1987), Lang and Lieb (1993), and also Lieb (2000). The two glaciers are mainly characterized by their small size (far less than 1 km^2), lack of distinct snow accumulation areas and partial debris cover (cp. also Figure 7).

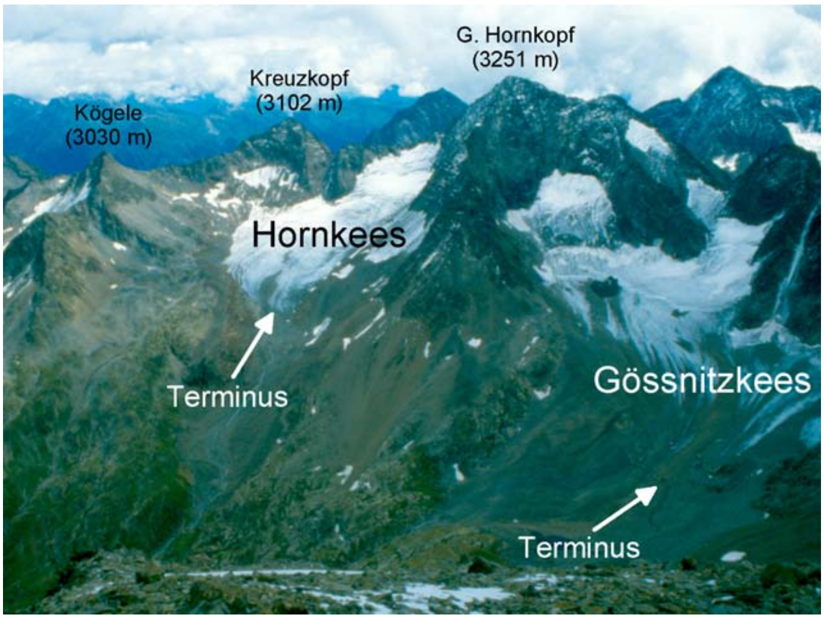

Figure 6. Terrestrial view of Gössnitzkees and Hornkees seen from Roter Knopf (3281 m). Viewing direction in southeasterly direction. Photograph taken by V. Kaufmann on 6 September 1983.

In 1982, glacier monitoring started at both glaciers with simple geodetic measuring methods by Gerhard Lieb and Viktor Kaufmann (Lieb and Kaufmann, 1985). The outline of the glacier terminus was measured by means of trilateration. Glacier length change was calculated based on the annual terminus positions measured (Lieb, 2000). The glacier history of both glaciers, from the Little Ice Age advance of 1850 up to the present (1997), was reconstructed in a research project funded by the Hohe Tauern National Park Fund (project leader Gerhard K. Lieb from the Institute of Geography and Regional Science, University of Graz). Various measuring techniques for glacier change assessment, such as aerial photogrammetry, terrestrial photogrammetry, geodetic methods, terrestrial laser scanning, and radar interferometry, have been applied at the Gössnitzkees test site over the course of the last 10 years.

Glaciologists are interested in the altitudinal change in glacier area and volume as a function of time. The latter parameter refers to glacier mass balance (Oerlemans, 2001). In the following, different aspects of glacier monitoring and also of visualization of glaciation and its temporal change will be addressed. Atmospheric warming has caused significant glacier retreat and subsequent surface height change in the Austrian Alps. Two glacier inventories (1969, 1998) have so far been carried out in Austria (Lambrecht and Kuhn, 2007).

Figure 7. Glacier terminus of Gössnitzkees. Supra-glacial debris is omnipresent in the lower part of the glacier. Photograph taken by V. Kaufmann on 15 September 1982.

4.2. Aerial photogrammetry

Aerial photographs provide very good support for glacier mapping (Kääb, 1996; Würländer and Eder, 1998; amongst others). At present, modern digital photogrammetric workstations are used in practical work (Kääb, 2005; Bauder et al. 2007). In the early stages of the research project mentioned previously, an analytical DSR-1 plotter of Kern was used for photogrammetric work. Photographs of six different glacial stages between 1954 and 1997 were acquired and photogrammetrically processed. Later on, aerial photographs of two additional younger glacial stages, 2002 and 2006, were added to the time series and processed digitally. Multi-temporal data sets consisting of orthophotos, DEMs, glacier boundaries, and other collateral information were input into a digital database for glacier studies (see Kaufmann and Plösch, 2000; cp. also Würländer and Eder, 1998).

4.2.1. Quantification of glacier retreat 1850-2006

A FORTRAN software tool was developed by the author for exploring the given database. The database includes not only aerophotogrammetric data but also glacier reconstructions based on field investigations and old maps (1929, 1873, and 1929). The glacier reconstructions were provided by experts of the Institute of Geography and Regional Science of the University of Graz (for details see Kaufmann and Plösch, 2001). The results of this glacier study are summarized in Kaufmann and Ladstädter (2008a). The main findings are given here: Gössnitzkees covered an area of 155.5 ha in 1850, and 58.9 ha in 2006; the corresponding values for Hornkees are 91.6 ha, and 30.6 ha, respectively. Both glaciers have lost almost 2/3 of their areal extent since 1850 (cp. Figure 8). The volumetric change for both glaciers was negative for all time intervals considered except for 1974-1983. These findings are in good agreement with results obtained from large-scale glacier studies in the European Alps (Haeberli et al., 2007). For both glaciers, the equilibrium line altitude (ELA) was estimated at approx. 3020 m for the period 1997-2006, which means that both glaciers were completely out of balance during the past decade. Net mass balance was negative for all altitudinal zones. Assuming the same amount of glacier melt for the future, both glaciers will disappear entirely in 20 to 25 years. Subsurface topography was reconstructed hypothetically. The thermal isolation effect of the supra-glacial debris was omitted in the calculation.

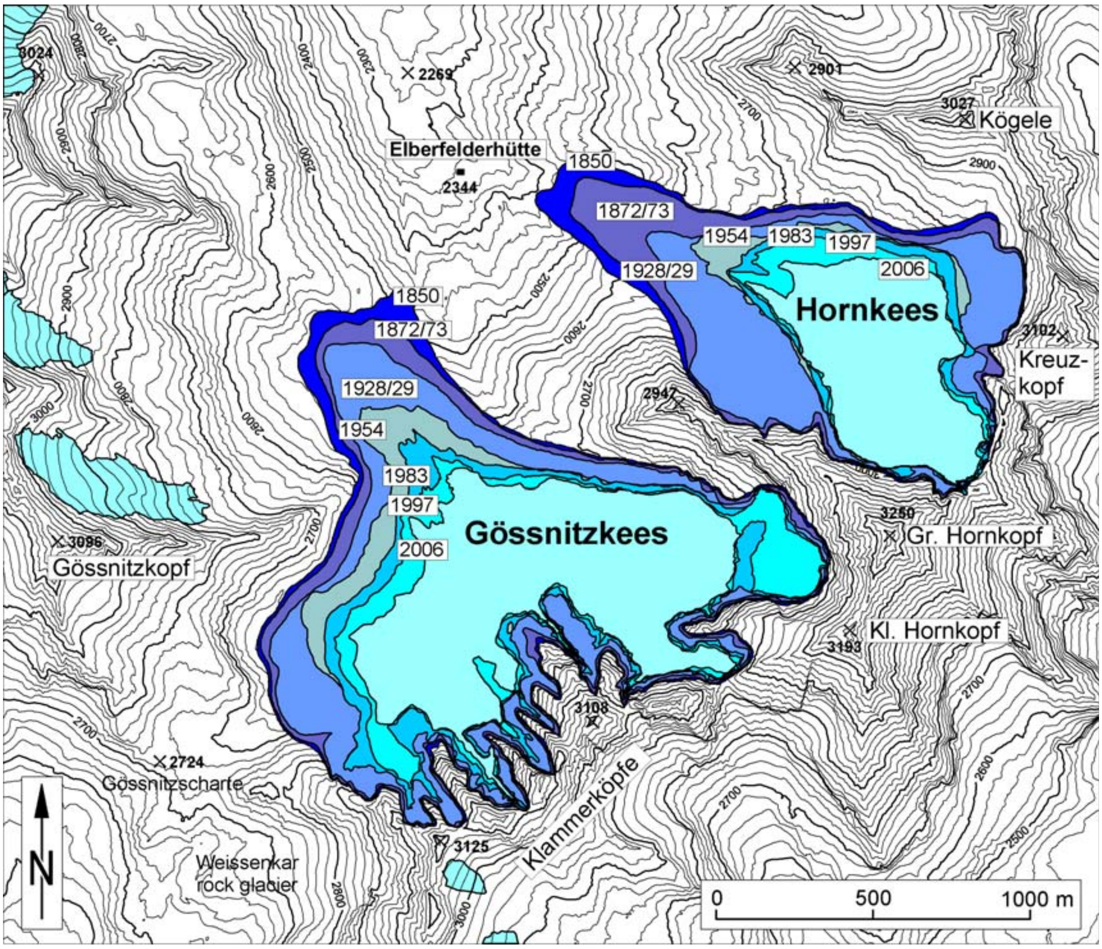

Figure 8. Thematic map showing the changes in area of Gössnitzkees and Hornkees since 1850 (modified after Kaufmann and Ladstädter, 2008a).

4.2.2. Visualization of glacier retreat

An orthophoto map "Gössnitz- and Hornkees, Schobergruppe" at 1:10,000 scale was published (GLACIER-Map, 1998, Appendix A13). A "glacier video" was produced with the support of the Computing Center of the Graz University of Technology, exemplifying the whole process of data capture, modeling, and quantification (Kaufmann, V. and Plösch, 2000; Kaufmann and Plösch, 2001). The spatio-temporal change of both glaciers is shown using computer animation. The animation software Maya of Alias|Wavefront was used to further process the key frames given in order to realistically visualize glacier change over time. The full-length video (12 min. 30 sec.) is included on the attached DVD (see Appendix B). Aspects of visualization of glaciers and glacier change are thoroughly discussed in Hurni et al. (2000) and Kääb et al. (2003). In this context, the author also refers the interested reader to the homepage (MountainCarto, 2009) of the Commission on Mountain Cartography of the International Cartographic Association (ICA).

4.2.3. Measurement of glacier flow velocity

Flow velocity describes the kinematic state of a glacier and is a good indicator of the glacier's thickness. Surface flow velocities are used in numerical modeling of glacier flow (Gudmundsson, 1994). Flow velocity can be measured both geodetically and photogrammetrically (see following sub-sections), and also interferometrically using radar image data (discussed in Chapter 6). In order to measure the surface flow velocity, for example of a glacier, distinct particles/objects of the surface have to be tracked over time. This can best be accomplished by automatic image matching (cp. Wangensteen et al., 2006). The concept of measuring 3D surface deformation in aerial photographs, to be explained in the next chapter, was also applied to Gössnitzkees. Since the surface of Gössnitzkees is debris-covered to a great extent, a dense field of flow vectors was obtained for most parts of the glacier (see Figure 9). Areas without stable texture over time did not produce any valid results. Points on bedrock are generally stable and do not move; they were used for checking purposes.

It is worth mentioning in this context that it was recognized during the course of this experiment that the digitized aerial photographs showed cyclic image distortions. These small errors were due to malfunction of the photogrammetric scanner used (Raster Master 1 of Wehrli). This problem could only be revealed through the high measuring precision of digital image matching.

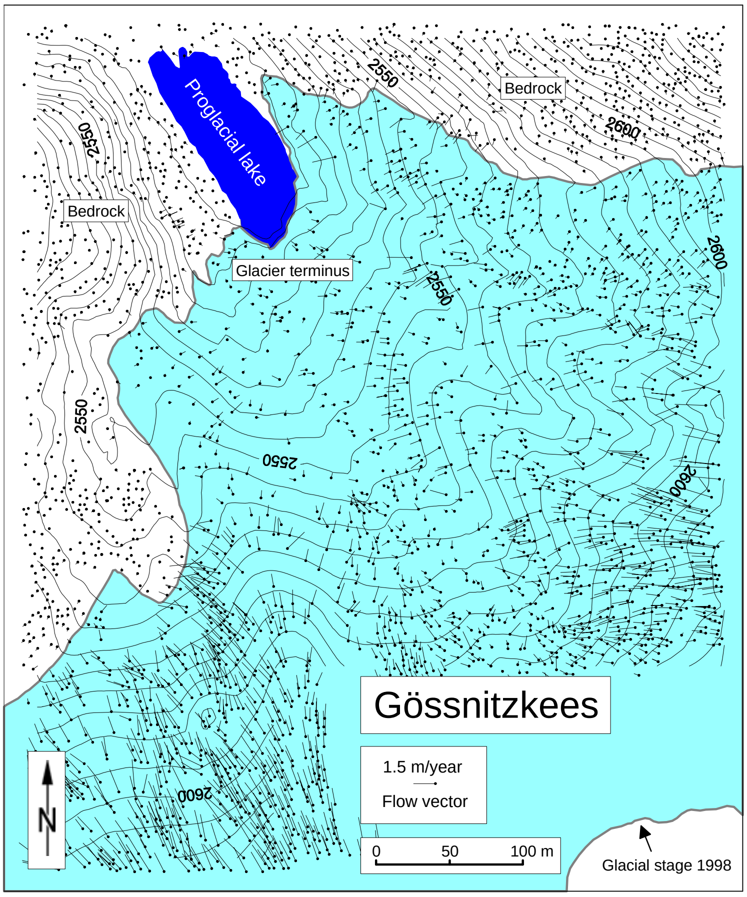

Figure 9. Field of horizontal flow vectors at Gössnitzkees for the time period 1997-1998. Flow vectors have been derived by automatic image matching.

4.3. Terrestrial photogrammetry

Terrestrial photogrammetry has had a long tradition in mountain cartography and glacier mapping (see in particular Rinner et al., 1972). Aerial surveys have almost completely replaced ground-based photogrammetric surveys. Terrestrial-photogrammetric mapping projects have been carried out only occasionally over the past two decades (references given in Kaufmann and Ladstädter, 2008b). Modern low-priced digital SLR cameras, however, suggest the rebirth of terrestrial photogrammetry for mapping projects in high mountain environments.

At Gössnitzkees, the author conducted a unique comparative study on the application of terrestrial photogrammetry to glacier monitoring, involving terrestrial-photogrammetric surveys (1988-2007) using both analog and digital cameras, such as Zeiss TAL phototheodolite, Rolleimetric 6006, Nikon D100, Hasselblad H2D-39, and Nikon D80. The results obtained are described in Kaufmann and Ladstädter (2004a) and Kaufmann and Ladstädter (2008b). Additionally, a Nikon D300 small-format digital camera with a 12 megapixel CCD sensor was used in 2008 (see Figure 10).

Figure 10. Terrestrial photograph of the central part of Gössnitzkees taken from the opposite slope where the photogrammetric baselines are located. Camera: Digital SLR Nikon D300, f=20 mm. Photograph taken by V. Kaufmann on 22 August 2008.

4.3.1. Pre-processing

The terrestrial-photogrammetric processing chain consists of (1) appropriate pre-processing of the image data and (2) photogrammetric evaluation. Depending on the image data available, the following pre-processing steps need to be carried out: analog-to-digital conversion (Zeiss TAL, Rolleimetric 6006), elimination of color fringes due to chromatic aberration (all digital cameras), elimination of lens distortion (all cameras, if applicable), correction for film unflatness and film distortion (Rolleimetric 6006), masking of réseau crosses for better visual perception (Rolleimetric 6006). Two computer programs (DistCorr and ReseauCorr; cp. Ladstädter and Kaufmann, 2004) were developed by the author's colleague and co-worker at the Institute, Richard Ladstädter. A prerequisite, of course, is the knowledge of the elements of inner orientation of the camera systems used. The idea of the concept given is to generate and finally work with "perfect" central-perspective images with the principal point located in the image center and without any kind of image distortions. Pre-processed (rectified) image data have proved to be very useful because they make performing inner orientation on a digital photogrammetric workstation less error prone. However, this pre-processing step is not mandatory.

State-of-the-art camera calibration using either a planar calibration target (of PhotoModeler) or a 3D test field (in-house available or of Microsoft Photogrammetry, Graz) was carried out at the author's institute (Fauner et al., 2008; for a general overview of digital camera calibration techniques see Remondino and Fraser, 2006).

Special attention was paid to the elimination of color fringes in the digital photographs caused by lateral chromatic aberration of the camera systems used (Kaufmann and Ladstädter, 2005). Modeling of chromatic aberration for high precision photogrammetry is also discussed in Cronk et al. (2006) and Luhmann et al. (2006). The elimination of the effect of chromatic aberration is a prerequisite for high-quality image measurements, precise image interpretation/classification, and for obtaining optimal orthophoto quality. At present, chromatic aberration correction is already routinely integrated in post-processing software of professional and also semi-professional digital cameras.

4.3.2. Photogrammetric evaluation

Only multi-temporal stereopairs were considered in the processing chain for ease of application. Practical work was carried out using an ImageStation of Z/I Imaging. Ground control points were geodetically measured during the field campaign of 2003. The Rolleimetric 6006 stereomodel of this campaign was photogrammetrically oriented using these points. In a next step, stable 3D reference points were measured in this reference model for absolute orientation of all other stereomodels. Multi-temporal DEMs with a grid-spacing of 2.5 m were interpolated from points measured in regular grid form and other features (additional surface points, break lines, glacier boundaries, etc.) extracted from the stereomodels. Glacier change was quantified numerically by subtracting multi-temporal DEMs providing surface height change and by overlaying glacier termini in order to retrieve glacier length change. The accuracy obtained was assessed by coincident geodetic measurements (see next sub-section).

4.3.3. Glacier monitoring using low-cost digital cameras

The annual surface height change of Gössnitzkees can be determined with an accuracy better than ±20 cm/year with all the small-format digital cameras investigated, although DEMs of individual epochs showed systematic offsets of variable size in the 10-centimeter range. Based on the photogrammetric data, a mean surface lowering of -1.51 m/year (longitudinal profile, 2530-2560 m) and a glacier length decrease of -87.6 m was calculated for the time period 1988-2007. Other results in numerical and graphical form are presented in Kaufmann and Ladstädter (2004a) and Kaufmann and Ladstädter (2008b).

The author has developed a workflow of how to use low-cost consumer cameras for glacier monitoring. This new concept is based on modern techniques (robust image matching, multi-ray geometry) of computer vision and is meant to support the Austrian Alpine Club in its annual glacier measurements (see Kaufmann and Ladstädter, 2008b).

4.4. Geodetic measurements at Gössnitzkees

A small geodetic network currently consisting of 10 stable reference points in the vicinity of the glacier terminus was set up in 1996 in close cooperation with the present Institute of Navigation and Satellite Geodesy, Graz University of Technology (Kienast and Kaufmann, 2004). Geodetic work has until recently been supported by the author's colleague Gerhard Kienast. Since 1996, the position of the glacier terminus, the surface height along two longitudinal profiles and 3D positions of 10 object points have been measured every year providing detailed geometric information on glacier length change, surface height change and glacier movement (see Figure 11). The geodetic measurements were also used for the validation of results obtained by terrestrial photogrammetry, as already indicated previously, and terrestrial laser scanning.

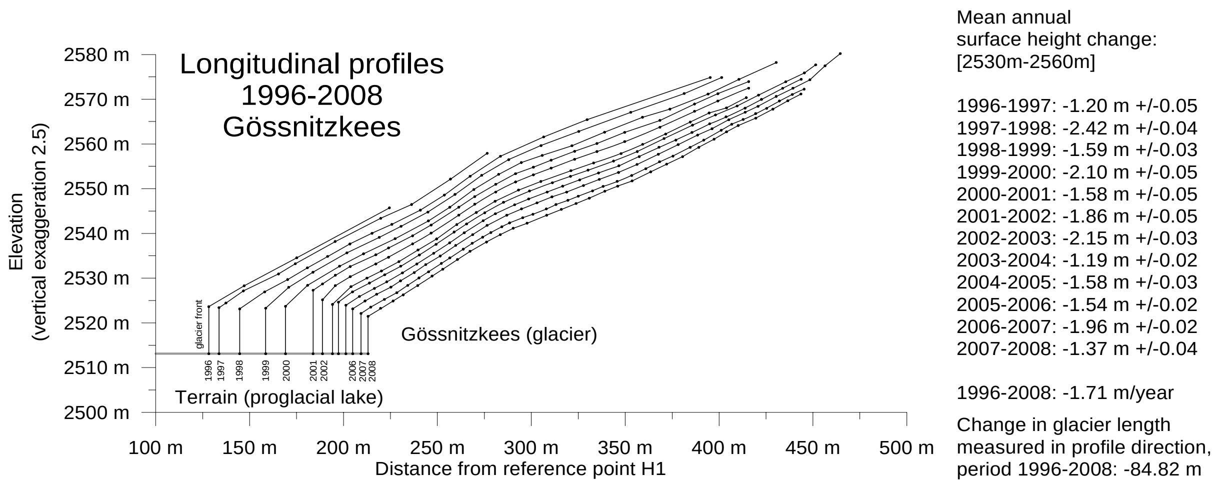

Figure 11. Graphical and numerical representation of glacier retreat of Gössnitzkees 1996-2008 shown for the central longitudinal profile.

4.5. Terrestrial laser scanning and differential SAR interferometry (DInSAR)

Terrestrial laser scanning is a powerful tool for surface reconstruction in close-range applications (Petrie and Toth, 2009). The Institute of Digital Image Processing of Joanneum Research Graz has gathered data at

Gössnitzkees over the past few years using a LPM-2k laser scanner of Riegl Laser Measurement Systems. Final results are still pending and the interested reader is therefore referred to Avian et al. (2007).

Kenyi and Kaufmann tried to retrieve glacier flow velocities over Gössnitzkees from interferometric ERS-1/2 SAR data. This attempt was not successful, however, because of the unfavorable imaging geometry of ERS-SAR in respect to mountainous terrain, temporal decorrelation of the radar data available, and small size of the glacier (cp. also with Section 6.5). The same radar data applied to Pasterze glacier, Austria's largest glacier, provided good results with, at least, one of the interferometric pairs (see Kaufman et al., 2005).

4.6. Acknowledgments

The "glacier video" was produced at Studio AV-Media, Central Informatic Services (CIS), Graz University of Technology. The support of both Peter Javurek and Reinhard Plösch is greatly appreciated.

5. Hochebenkar rock glaciers (North Tyrol, Austrian Alps)

5.1. Introduction to permafrost and rock glacier research

Permafrost is lithosphere material that permanently remains at or below 0°C. The time span of continuous frost must be two or more consecutive years for permafrost conditions to prevail (Haeberli et al., 2006). Permafrost is, for example, permanently frozen rock. Permafrost must not be confused with glaciers, which belong to the hydrosphere. Permafrost can be found at high latitudes, i.e. Arctic and Antarctic, and also in high mountains at low and mid-latitudes. Mountain permafrost is bound to mountainous terrain and its characteristics (Gruber and Haeberli, 2009). Ebohon and Schrott (2008) have elaborated a new permafrost map of Austria showing areas of possible and probable (mountain) permafrost distribution in the Alps.

Ongoing global warming is also affecting mountain permafrost with traceable impact on mountain environments, such as increasing rock fall caused by destabilized rock faces (Harris et al., 2003; Haeberli and Gruber, 2008 and 2009).

Rock glaciers are creep phenomena of mountain permafrost composed of rocks and interstitial ice. Active rock glaciers creep downslope by force of gravity due to internal deformation of the ice. Sliding may also be possible at certain shear horizons. Due to the above mentioned processes, the surfaces of rock glaciers often show characteristic flow features, such as furrows and ridges, reminiscent of lava flows. Rock glaciers are an important mass transport system in mountainous/alpine regions. Barsch (1996) and Haeberli et at. (2006) can serve as starting points for further reading. The origin of rock glaciers is still a matter of debate (a concise synthesis is given in Gasselt, 2007, chapter 3).

The morphodynamics of rock glaciers is still not sufficiently understood because of a lack of process understanding and information from inside the creeping permafrost body (cp. Arenson et al., 2002; Ladanyi, 2003; Kääb and Weber, 2004). Surface deformation of a rock glacier can be measured by various observation techniques (good overview given in Kääb, 2008), the most important of which will be described in this treatise. In the following, the words flow and creep are used synonymously when not otherwise indicated.

A comparative study (Delaloye et al., 2008) analyzing the mean annual flow velocities of 16 different rock glaciers in the European Alps for the observation period (1999-2007) revealed that the surface flow velocities observed are to a great extent synchronous, and inter-annual changes are mostly well correlated with mean annual air/ground temperature, but with a time delay of several months. The reader interested in modeling permafrost creep is also referred to Kääb and Reichmuth (2005), Kääb et al. (2007), and Frauenfelder et al. (2008).

It is assumed that climate change has an impact on rock glacier dynamics, and a respective climate signal can be deducted from long-term flow velocity measurements. Recent results obtained from the author's rock glaciers, including results addressing surface height change, will be shown and discussed in the following sections.

The phenomenon of rock glacier disintegration has also been observed on some rock glaciers in the European Alps during the past few decades, with the development of crevasse-like tension cracks (cp. Roer et al., 2008 and Kääb, 2008) and collapsing surfaces (cp. Krysiecki, 2008). Two examples, i.e. Outer Hochebenkar rock glacier and Hinteres Langtalkar rock glacier, will be presented in this treatise to highlight this phenomenon.

Rock glacier monitoring has a comparatively long history in Austria, commencing as early as the 1920s (Pillewizer, 1957; Vietoris, 1972; review paper by Kaufmann, 1996; Schneider and Schneider, 2001; Krainer and Mostler, 2006). More recent references will be provided later on in the paper.

The main focus of all rock glacier studies to be presented in this treatise is to measure surface flow velocity and surface height change, both being important geomorphometric parameters used in climate change studies. Recently, Embleton-Hamann (2007) has outlined that mountain permafrost degradation in Austria could increasingly trigger geomorphological hazards.

5.2. Geographical setting and background information

The Hochebenkar rock glaciers comprise of two rock glaciers, i.e., the Inner (in German *Inneres*) and Outer (in German *Äußeres*) Hochebenkar rock glacier, located in two adjacent cirques of the Ötztal Alps (Haeberli and Patzelt, 1982; Patzelt et al. 2007). The study area is centered at 46°50'N, 11°01'E. Computer generated overflights of both glaciers are available for inspection, see Appendix B. Outer Hochebenkar rock glacier (see Figure 12) is characterized by an interesting topographic situation. The rock glacier tongue (total length of approx. 1100 m) has advanced, starting from a low inclined cirque floor, over a break into steeper terrain. Sliding processes occurred at the lower section of the rock glacier causing relatively high annual flow velocities in the meter-range (see time-lapse photography of Outer Hochebenkar rock glacier, Appendix B) and subsequent disintegration of this part of the rock glacier. Inner Hochebenkar rock glacier shows traces (fluted moraines) of former glaciation on its surface. Remnants of recent glaciation are still visible at the rooting zone of Inner Hochebenkar rock glacier (see Kaufmann and Ladstädter 2002a, Figure 3).

Outer Hochebenkar rock glacier is well known to the scientific community because of its remarkably long record of geodetic and photogrammetric measurements starting in the 1930s (overview given in Kaufmann and Ladstädter, 2002a). Source references are Pillewizer (1957), Vietoris (1972) and Schneider and Schneider (2001). Additional photogrammetric work carried out by the author and his colleague Richard Ladstädter is outlined in the remaining sections of this chapter. Geodetic measurements are still carried out annually by Heralt Schneider (University of Innsbruck). Rott and Siegl (1999) were the first researchers to apply differential SAR interferometry (DInSAR) in rock glacier research. They succeeded in analyzing the motion of Outer Hochebenkar rock glacier using ERS-1 and ERS-2 SAR images.

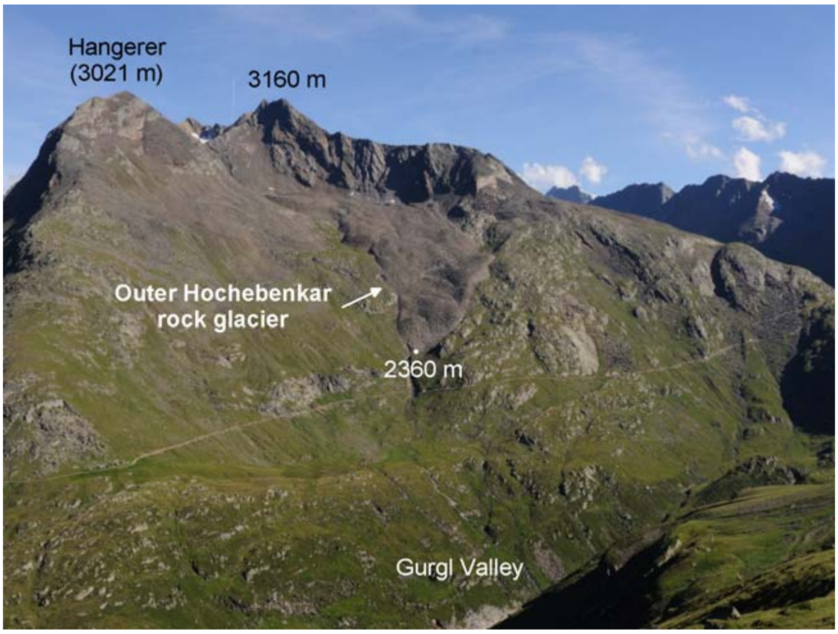

Figure 12: Terrestrial view of Outer Hochebenkar rock glacier towards southeast. Photograph taken by V. Kaufmann on 10 August 2008.

5.3. Photogrammetric measurement of 3-D displacement vectors using digital quasi-orthophotos

The concept of automatic measurement of 3D displacement/flow vectors in digital multi-temporal photographs for rock glacier studies has already been formulated in Kaufmann (1998b). The concept outlined is based on the work of Baltsavias (1996) although a similar approach was presented earlier by Schenk et al. (1990). The interested reader is also referred to other publications dealing with the same problem of correcting both DEMs and/or digital orthophotos applying image matching techniques, for example, Norvelle (1996), Krupnik and Schenk (1997), and Höhle and Potucková (2005).

The basic concept of using pre-rectified image patches for digital image matching of oriented stereopairs was developed by the author in 1982/83 (Kaufmann, 1983). Image matching was still carried out in image space. The image content of the right stereo partner was re-projected into the left stereo partner using an iteratively improved DEM. Image matching was performed using the normalized cross-correlation function with sub-pixel interpolation. The surface in object space was approximated by a best-fitting plane. The algorithm was implemented in FORTRAN on a computer PDP 11/34 using a dedicated high-performance DeAnza IP5000 image array processor.

The basic principle of the previously mentioned concept is that particle tracking in multi-temporal photographs is not done in the original image space but in object space using quasi-orthophotos. Quasi-orthophotos are generated using approximate/preliminary DEMs. A prerequisite is the proper exterior orientation of all image frames. The procedure outlined is not restricted to aerial photographs at all, but can also be applied to any other imaging geometry, for example, that of satellite-based optical data (cp. Yeu et al., 2000 and Raggam et al., 2005). All technical aspects of this mapping technique are described in Kaufmann and Ladstädter (2002b and 2003). Ladstädter has developed this concept further and also provided a software tool (ADVM 2.0) for practical applications (Kaufmann and Ladstädter, 2004b). The algorithms implemented comprise geometrically constrained least-squares matching, multi-ray geometry, a hierarchical procedure, and point selection using the Förstner interest operator. The computation of displacement vectors is stringent from a photogrammetric point of view.

Vollmer (1999) has developed a similar program, called CIAS (Correlation Image Analysis System), at the Institute of Geography, University of Zurich. His concept is based on the assumption that the digital terrain models used are already perfect and of high quality (see also Kääb, 2005, for practical examples).

Both concepts by Kaufmann and Vollmer propose to eliminate the remaining systematic errors using stable regions where computed 3D displacement vectors are supposed to be zero.

The proposed concept of measuring 3D displacement vectors using digital quasi-orthophotos was not only applied successfully to various Austrian rock glaciers but also to a debris-covered glacier, as already mentioned in Chapter 4, and to a landslide area (see Chapter 10).

Aerial photographs from eight different epochs between 1953 and 1997 covering both Hochebenkar rock glaciers were evaluated in that study. Full details on the photogrammetric processing (see Kaufmann and Ladstädter, 2002) and the results obtained have already been published (Kaufmann and Ladstädter, 2002b, 2003 and 2004b). This study was also characterized by the transition from analytical to digital photogrammetry. While photogrammetric orientation (all stereomodels) and feature extraction (1953 and 1997) was still carried out using an analytical plotter, subsequent work, including orthophoto production and computation of 3D displacement vectors, was fully accomplished in the digital domain. Quantitative information on surface flow velocity and surface height change were retrieved from the multi-temporal data. This information is provided area-wide for both glaciers except for the lower end of Outer Hochebenkar rock glacier, where large mass movements had occurred throughout the time, which hampered the successful tracking of surface points. The results obtained at Outer Hochebenkar rock glacier agree very well with the findings of Schneider and Schneider (2001) obtained from long-term geodetic measurements (1951-1999). Nevertheless, a few remarks will be presented in this paper.

5.4. Horizontal flow velocity

A first attempt to quantify the kinematic state of Outer Hochebenkar rock glacier using both an airborne (1997) and a terrestrial stereopair (1986, see also next Section 5.6) was accomplished by former student Bernhard Rieder. He traced the movement of 12 distinct rocks/boulders of the rock glacier surface in both stereomodels obtaining maximum horizontal flow velocities of up to 1.25 m/year (cp. Kaufmann, 1996). This is to be compared with Pillewizer (1957), who measured maximum flow velocities up to 3.57 m/year for the time period 1953-1955. The large flow velocities of the 1950s were never to be reached again, as proved both photogrammetrically (this study) and geodetically (Schneider and Schneider, 2001). During the 1970s and 1980s the creep of Outer Hochebenkar rock glacier was retarded. A marked speed-up of rock glacier movement was again observed during the 1990s, reaching a maximum flow velocity of up to 1.1 m/year, which was photogrammetrically determined for the time period 1990-1997. The upper part of the rock glacier is creeping at velocities of up to 30 cm/year. Schneider and Schneider (2001) have found out that short-term inter-annual changes of flow velocities correlate to a high degree with mean annual air temperatures of nearby meteorological stations, obviously with a time-lag of less than one year (cp. recent results presented by Delaloye et al., 2008).

The flow/creep pattern of Inner Hochebenkar rock glacier is completely different from its northern neighbor. Two active regions with maximum mean flow velocities of up to 40 cm/year (1953-1997) were identified (cp. Kaufmann and Ladstädter, 2002a, Figures 8 and 9). The central part in between the two active zones does not show any significant movements for the time span given (for reasons of comparison see also Figure 13, this publication). The results obtained for the other time periods, which have not yet been published, correspond very well with the findings of Schneider and Schneider (2001) presented previously.

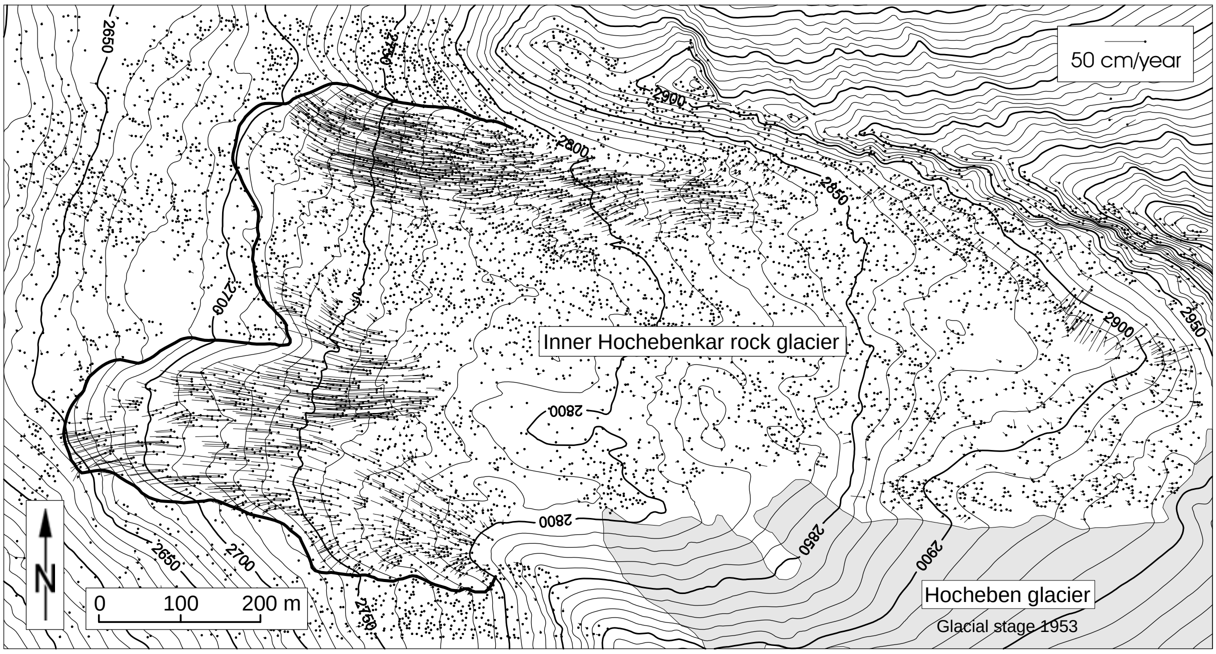

Figure 13: Flow vector field at the Inner Hochebenkar rock glacier for the time period 1953-1969. Maximum flow velocities of up to 56.1 cm/year were measured, being the highest values recorded ever since on this rock glacier. 7491 flow vectors were determined by means of digital image matching.

5.5. Surface height change

Information on surface height change can be derived by subtracting multi-temporal digital elevation models. Color-coded maps visualizing the change provide a better understanding of the mass movement. Climate-induced permafrost degradation and subsequent surface height lowering is difficult to estimate since the amount of the latter is quite small, most likely in the range of several cm/year, and the climatically induced surface lowering is hard to distinguish from the kinematically induced surface height change. Mass balance analyses were carried out based on the method developed for Gössnitzkees and Hornkees (see Section 4.2.1). The difference DEM for 1953-1997 of both rock glaciers did not reveal any significant volumetric changes as far as photogrammetric accuracy is concerned, despite the long observation period (44 years), high accuracy of DEMs due to manual photogrammetric mapping, and completeness of 3D data capture.

The evaluation of the aerial photographs of 2004 is still pending.

5.6. Terrestrial photogrammetry applied to Outer Hochebenkar rock glacier

As already outlined in Section 4.3, terrestrial photogrammetry was successfully applied at Gössnitzkees glacier. The main task at Gössnitzkees was to measure the glacier’s surface height change. Horizontal flow velocity was not addressed because of the relatively poor base-to-distance ratio of the imaging geometry. The aim of another experiment at Outer Hochebenkar, however, was to investigate the applicability of the previously outlined 3D measurement technique based on quasi-orthophotos to the terrestrial case (Ladstädter and Kaufmann 2004; Ladstädter and Kaufmann, 2005). It was indented to measure 3D displacement vectors of distinct surface points over time. Four camera systems were used: Zeiss Photheo 19/1318, Linhof Metrika, Rolleimetric 6006, and a Nikon D100. Photographs were taken in 1986, 1999, and 2003. Another revisit was made in 2008, but the digital photographs taken with a Nikon D300 have not yet been considered in this study. All photographs were pre-processed following the procedure described in Section 4.3.1. The absolute orientation of all terrestrial stereomodels was accomplished using ground control points derived from aerial photographs. In a further step, all 21 image frames were pre-rectified using a preliminary digital terrain model of the project area. The vertical projection plane for deriving the quasi-orthophotos was selected orthogonal to the mean viewing direction. The benefit of this procedure is obvious: the warped photographs look very similar to one another geometrically (cp.

Figure 14) and automatic image matching using ADVM software was thus facilitated to a great extent. Digital elevation models for each epoch and 3D displacement vectors describing the surface deformation could be derived from the object points obtained. Figures 7 and 8 of Ladstädter and Kaufmann (2005) present the horizontal flow vectors derived for two different time periods, 1986-1999 and 1999-2003. Surface points located outside of the rock glacier were used for both quality check and accuracy assessment. For both time intervals, a root mean square error of ±60 cm in horizontal vector length was achieved, resulting in accuracies of ±5cm/year and ±15cm/year, respectively. The isotachs computed confirm the recent increase in flow velocities of up to 2.3 m/year.

Vertical height accuracy is in the sub-pixel range of the original image data. The horizontal flow component, however, suffers from the unfavorable quadratic error law of terrestrial photogrammetry in viewing direction and the result is, therefore, inhomogeneous to a certain extent. Since the imaging geometry of ground-based photogrammetry is basically controlled by the given topographic situation, the achievable geometric accuracy is variable.

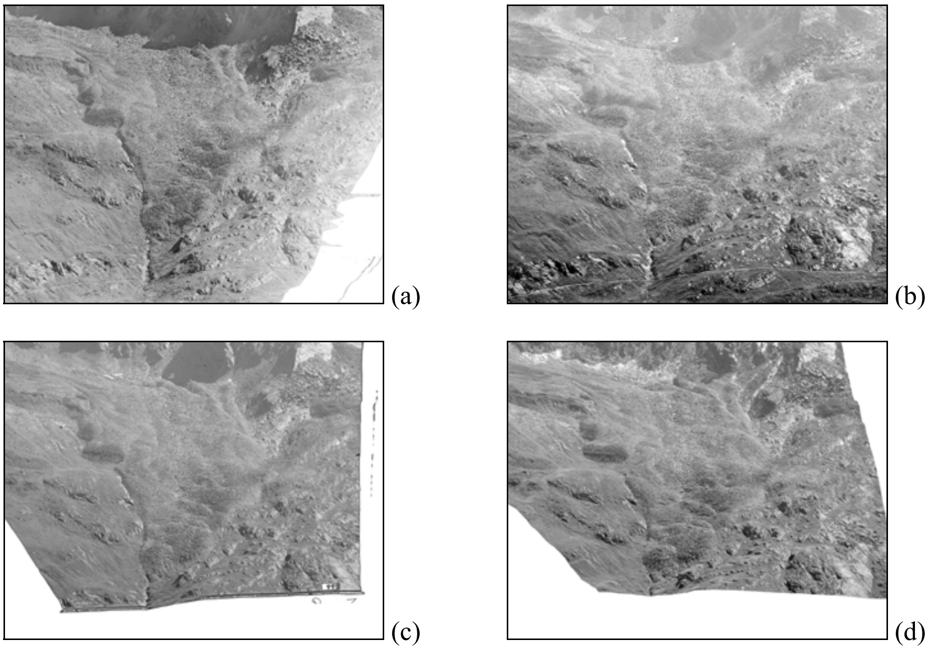

Figure 14: Multi-temporal quasi-orthophotos derived from photographs taken with (a) Zeiss Photheo 19/1318, 1986, at camera position no. 1, (b) Linhof Metrica, 1999, camera position no. 2, (c) Rolleimetric 6006, 1999, camera position no. 4, and Nikon D100, 2003, camera position no. 6.

5.7. Visualization of the kinematics of the Hochebenkar rock glaciers

As already indicated, the quasi-orthophotos (both aerial and ground-based) obtained in this study are very congruent and can therefore be used for the generation of computer animations visualizing flow, creep, and sliding processes of the rock glacier, irrespective of their parameters of exterior orientation and elements of inner orientation. Please see DVD attached to this treatise, which also holds a “rock glacier video” (length 5 min. 6 sec.) produced to document the kinematics of both rock glaciers from 1953-1997.

5.8. Acknowledgments

I am indebted to Robert Kostka, Institute of Photogrammetry and Remote Sensing, Graz University of Technology, who introduced me to rock glacier research. Kostka also organized the first two field campaigns to Outer Hochebenkar rock glacier during which I had the privilege to be his co-worker. The support of Gernot Patzelt, head of the former Institute of High Mountain Research, University of Innsbruck, during three field work campaigns is very much appreciated. The “rock glacier video” was produced at Studio AV-Media, Central Informatic Services (CIS), Graz University of Technology. The support of both Peter Javurek and Reinhard Plösch is once again greatly appreciated.

6. Doesen rock glacier (Carinthia, Austrian Alps)

6.1. Introduction and geographical setting

Gerhard K. Lieb, Institute of Geography and Regional Science, University of Graz, investigated mountain permafrost in the Eastern Austrian Alps within a multidisciplinary research project (P 09565-GEO) funded by the Austrian Science Fund (FWF). He compiled a rock glacier inventory of the Eastern Austrian Alps consisting of 1451 rock glacier (complete inventory listed in Lieb, 1996; cp. also Lieb, 1998). The inner Doesen valley of the Ankogel Group, Hohe Tauern Range, was selected as a test site for detailed permafrost studies and field investigations. Doesen rock glacier (46°59'12"N, 13°17'08"E) is situated at the head of inner Doesen valley. This prominent tongue-shaped landform has a length of about 1000 m and a width of between 150 and 300 m (see Figure 15). Further geographical and morphological details on the test site and the rock glacier are given in Lieb (1996, 1998). Computer animations (repeat aerial photographs) showing the differential movement of Doesen rock glacier are provided on the DVD attached (Appendix B).

Various geophysical soundings, such as seismic, geoelectric, electromagnetic and ground penetrating radar surveys, have been conducted at Doesen rock glacier (further references are given in Lieb, 1996). The author was invited to prepare large-scale topographic maps of the area of interest and to augment the interdisciplinary work with metric information on the rock glacier kinematics. A long-term monitoring program on Doesen rock glacier was initiated within a research program financed by the Hohe Tauern National Park Fund. The program was carried out by the author's institute in close co-operation with the Institute of Navigation and Satellite Geodesy, Graz University of Technology, with substantial assistance of co-worker Gerhard Kienast. In the course of time (1995-2008) different geodetic, photogrammetric and remote sensing based observation techniques were investigated and developed further, building the foundations of the long-term monitoring program already mentioned. Later on, the long-term program was expanded by the author to other test sites in the Hohe Tauern Range, i.e., Hinteres Langtalkar rock glacier and Weissenkar rock glacier.

This chapter will address cartographic work, geodetic and photogrammetric surveys and the application of differential SAR interferometry, all related to Doesen rock glacier.

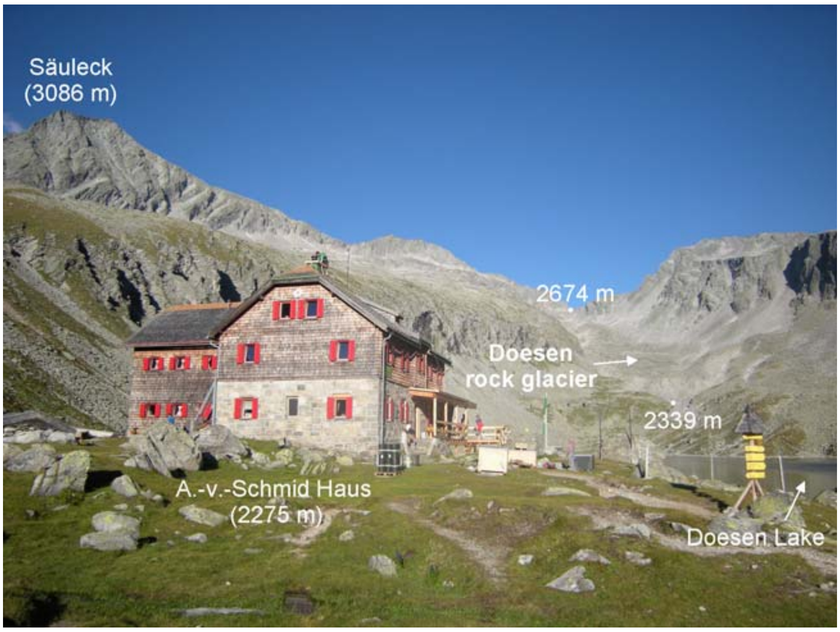

Figure 15: Terrestrial view of Doesen rock glacier. Viewing direction to the east. Photograph taken by V. Kaufmann on 19 August 2008.

6.2. Cartographic work

An orthophoto map 1:10,000, a relief map 1:10,000, a stereo- orthophoto map 1:30,000, and a stereo-orthophoto map 1:5,000 of the Doesen rock glacier were produced as a topographic basis for detailed studies (please see maps attached to Kaufmann, 1996, Appendix A17, or Kaufmann and Heiland, 1998). Relief and surface features were captured using an analytical DSR-1 plotter of Kern. The high-resolution orthophotos were generated using GAMSAD software developed by the author at the present Institute of Digital Image Processing, Joanneum Research Graz, in the early 1980s (for details see Kaufmann, 1984). The high geometric quality of the orthophoto map 1:10,000 can be visually checked, for example, at each perennial snow patch where the photogrammetrically captured borderline fits perfectly well its counterpart in the orthophoto. It should also be mentioned that perennial snow patches are good indicators of (discontinuous) permafrost in mountain environments. A multitude of multi-temporal orthophotos and digital terrain models were generated in the course of project work.

6.3. Geodetic measurements

In 1995, a geodetic network consisting of seven stable reference points made of brass was established under the leadership of G. Kienast. Technical details on the geodetic network can be found in Kienast and Kaufman (2004) and Kaufmann et al. (2007). GPS-based measurements were carried out to link this network with the Austrian Gauss-Krüger coordinate system. 34 object points were fixed on the surface of the rock glacier also using brass bolts (see Figure 16). Additional 107 points were selected along two transversal and two longitudinal profiles for better capturing surface flow patterns. Geodetic measurements of all object and profile points have been conducted every year since 1995, with one interruption in 2003 (cp. Kaufmann et al., 2007, and Kaufmann, 2009). The mean annual horizontal movement of Doesen rock glacier for the time period 2007-2008 is shown in Figure 16. The highest ever measured flow velocity was 45.6 cm/year for 2002-2004, determined right in the center of the rock glacier (point number 15). A comprehensive summary of the kinematic state of Doesen rock glacier in respect to horizontal flow/creep velocity is given in Figure 17. This figure also includes data derived from aerial photogrammetry. Relying on the same assumptions concerning rheology of the rock glacier (Kääb, 2005, chapters 2 and 9), surface lowering due to permafrost degradation was estimated at -2 to -2.5 cm/year. Multi-year flow/creep velocity data of rock glaciers can be also used to study the impact of atmospheric warming (addressed in more detail in Chapter 9).

High-precision geodetic measurements using a total station are time-consuming and costly if done in a high mountain environment. GPS measurements at object points were discontinued at Doesen rock glacier, since in several instances no valid solutions could be determined due to obstruction of the satellite signals by the surrounding mountains. An alternative to in-situ geodetic measurements are image-based remote sensing methods. Aerial photogrammetry is one of the most powerful methods in this respect and will be discussed below.

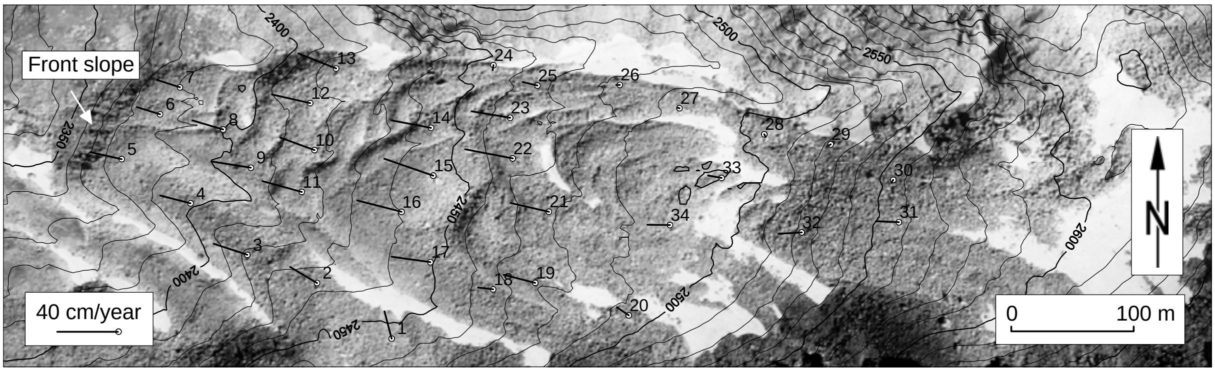

Figure 16: Mean annual horizontal movement of the 34 points marked with brass bolts on the Doesen rock glacier for the time period 2007-2008. Orthophoto of 15 October 1993.

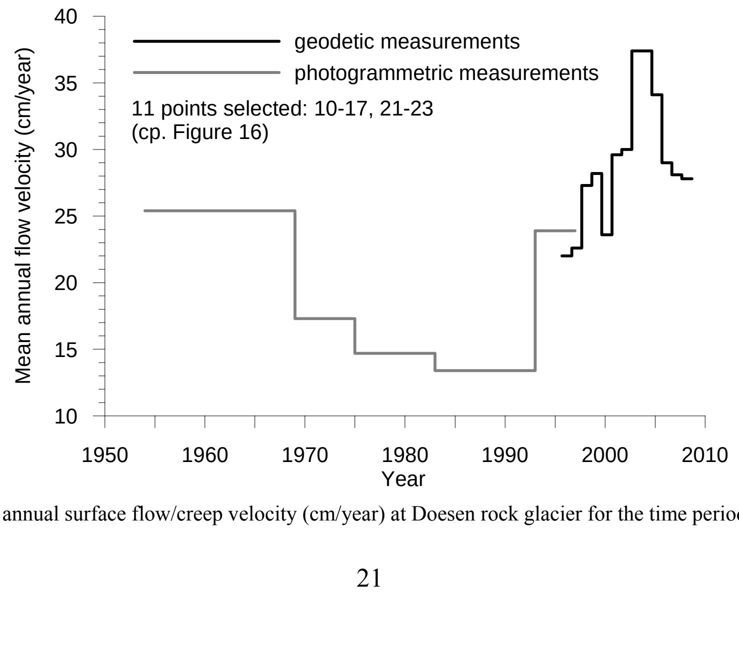

Figure 17: Change in mean annual surface flow/creep velocity (cm/year) at Doesen rock glacier for the time period 1954-2008.

6.4. Photogrammetric measurements

The possibilities of flow velocity measurement of rock glaciers using aerial photographs are outlined, for example, in Kääb (2005, pp. 70-76, p. 81) and Kaufmann and Ladstädter (2007a). At Doesen rock glacier two different workflows have been elaborated, i.e., interactive feature tracking in independent multi-temporal stereomodels using an analytical plotter (to be explained in the next sub-section) and automatic feature tracking based on digital quasi-orthophotos (as explained in the previous chapter).

6.4.1. Classical approach of photogrammetric mapping

Since stereoscopic point transfer between multi-temporal aerial photographs was not possible on our analytical DSR-1 plotter of Kern because of excessive differences in image scales, it was decided to measure prominent points, for example large boulders, in the different stereomodels. Over 600 distinct points evenly distributed over the rock glacier surface were selected for change detection. The rather difficult identification process was facilitated by prediction using previous point measurements. Appropriate software was developed by the author. The results obtained are presented in Kaufmann (1996, see map 1:5,000 "Fließbewegungen") and Kaufmann (1998c). This somewhat tedious work caused the author to develop a more comfortable solution using techniques of digital photogrammetry (Kaufmann, 1998b).

6.4.2. Digital photogrammetry and automation

The digital photogrammetric workflow has already been outlined in Section 5.3. Recapitulating, the workflow presented suggests performing basic photogrammetric tasks, such as image triangulation and orthorectification, on a digital photogrammetric workstation (DPW), and carrying out automatic measurements of 3D (or 2D) displacement vectors using additional software outside the DPW. A digital photogrammetric workstation ImageStation of Z/I Intergraph and the ADVM software of R. Ladstädter were used in this and all other subsequent projects not yet presented in the framework of this paper. Results obtained for Doesen rock glacier are presented numerically and graphically in Kaufmann et al. (2007) and Kaufmann and Ladstädter (2007a). Finally, it was also possible to compare and evaluate results obtained from both the classical/interactive and digital/automated approach. The results were considered to be identical from a statistical point of view. However, the fully digital approach is much faster, and what is particularly advantageous, it offers the opportunity to measure thousands or even ten thousands of 3D displacement vectors, which can support reliability to a great extent.

6.5. Differential SAR interferometry (DInSAR)

Space-borne SAR data was used to stereoscopically derive 3D topographic information of the Earth's surface in Section 3.5. The evaluation scheme outlined used only the amplitude/intensity of the SAR signal to retrieve surface height information. Principles of classical radargrammetry were applied. The measured SAR echo normally also comprises the phase information of the registered coherent signal. Phase information of two or more SAR scenes covering the same area can be exploited to obtain the surface height of the Earth's surface and its temporal change by means of interferometric techniques. The interested reader is referred to, for example, Bamler and Hartl (1998), Madsen and Zebker (1998), and Lu et al. (2007).

Space-borne DInSAR is a powerful technique for detecting and quantifying small deformations of the Earth's surface. It also allows surface flow velocities, for example of glaciers, to be measured. The start of ERS-1 in 1991 and ERS-2 in 1995 gave a boost to interferometric applications of SAR data. A vast amount of literature documenting these applications is available. A special application is the detection of mass movements, for example of landslides, in high mountain environments (Nagler et al., 2002b; Rott et al., 2003; Strozzi et al., 2005).

Space-borne DInSAR can also support permafrost and rock glacier research. Small surface deformations caused by differential frost heave and thaw settlement in arctic regions and creep of rock glaciers were successfully detected and also quantified (cp. Rott and Siegl, 1999; Wang and Li, 1999; Nagler et al., 2002a; Rignot et al., 2002; Kenyi and Kaufmann, 2003a; Strozzi et al., 2004).

Information on the European Remote Sensing Satellites (ERS-1/2) can be retrieved from ESA_ERS (2009).

Five ERS-1/2 SAR single-look complex (SLC) datasets covering Doesen rock glacier were provided by the European Space Agency (ESA) in the framework of an announcement of opportunity. These datasets were acquired in the time period 1992-1997. The interferometric processing chain for the present dataset is outlined in detail, e.g., in Kenyi and Kaufmann (2003b). One interferometric pair with high coherence was processed. Relief corrected phase shifts were converted to radar line-of-sight displacements. The maximum deformation measured in the DInSAR (differential interferometric SAR) map was about -18 mm/35 days. The surface deformations obtained were cartographically shown in 1-mm displacement isolines nicely revealing the spatial pattern of surface deformation of the rock glacier. A complementary orbit would be useful in order to better decompose the DInSAR-measured surface deformation into more meaningful geometric information for subsequent attribution to the different processes. Constraints for the successful monitoring of glaciers and rock glaciers using ERS-1/2 SAR data in a European alpine environment were elaborated in a follow-on project funded by the Hohe Tauern National Park Fund (Kaufmann et al., 2007, and project report Kaufmann et al., 2005).

Another successful application of ERS-1/2 SAR differential interferometry was demonstrated for Pasterze glacier, Austria's largest glacier. Mean horizontal surface flow velocities of up to 45-50 m/year were estimated from a one-day interferogram of 20/21 August, 1995 (Kaufmann et al., 2005).

Based on the experiences gained from practical studies applied to rock glaciers, it can be concluded that ERS-1/2 SAR differential interferometry is a useful tool for area-wide detection of surface deformation, however, preferably in a qualitative way only. Other methods than SAR differential interferometry have to be applied at a local scale to obtain quantitative information on surface deformation (cp. Delaloye et al., 2007, and Lambiel, 2008).

6.6. Outlook

Digital image data from digital aerial cameras (large-format as well as medium-format) and new algorithms developed by the computer vision community give rise to new possibilities in image-based rock glacier monitoring. Stringent use of multi-ray geometry (no more obligation to the stereo case for point reconstruction) and robust image matching (stable feature tracking in scale- and rotation-variant images) are prerequisites for fully automated change detection in remotely sensed data acquired by earth-bound, airborne, or space-borne sensors. New high-resolution satellite-based SAR systems, such as TerraSAR-X, are already in orbit and will provide new opportunities in terms of operational data analysis, also applied to rock glacier studies.

6.7. Acknowledgments

The interferometric processing of the SAR data was carried out by Lado W. Kenyi using RSG software of the Institute of Digital Image Processing, Joanneum Research Graz. The kind cooperation of Lado Kenyi is greatly appreciated. Special thanks are extended to Regina Heiland and Hans Peter Tilg, both former students and project co-workers, for their support during the initial phase of the rock glacier monitoring project.

7. Hinteres Langtalkar rock glacier (Carinthia, Austrian Alps)

7.1. Introduction and geographical setting

In contrast to Doesen rock glacier, Hinteres Langtalkar rock glacier is entirely different in its kinematics. It is a very fast moving rock glacier with flow velocities of up to 2 m/year and its physiognomy and morphodynamics relate very much to Hochebenkar rock glacier (described in Chapter 5).

Hinteres Langtalkar rock glacier (46°59'11"N, 12°46'54"E; Schober Mountains, Hohe Tauern Range) is situated in a glacially shaped cirque surrounded by mountain crests up to 3000 m high and is composed of a tongue-shaped main lobe, approx. 850 m long and stretching down to 2460 m, and a minor, though strongly wrinkled lobe in the rooting zone (see Figure 18). The rock glacier is located approximately 1500 m north of Hornkees. For more detailed information on the geographical setting of the rock glacier, the interested reader is referred to Krainer and Mostler (2001), Lieb et al. (2004), Avian et al. (2005), and Kellerer-Pirklbauer and Kaufmann (2007).

The topographic situation of Langtalkar rock glacier is shown in the orthophoto map "Blockgletscher Hinteres Langtalkar – Luftbildkarte 1:5 000" attached to the publication of Kaufmann (2004a). Please see Appendix 21. The rock glacier was most probably covered by a small glacier in the rooting zone during the Little Ice Age cold period of the mid-19th century. Evidence is given by lateral moraines left behind by the glacier on top of the rock glacier surface and clearly recognizable in aerial photographs (see references cited in the previous paragraph). This rock glacier, like many other rock glaciers, has a characteristic depression in the rooting zone. Most notable is the ongoing disintegration of the rock glacier. Marked surface ruptures and crevasse-like structures have developed during the last 50 years due to prevailing high-strain rates. Flow/creep velocities are increasing from the rooting zone towards the frontal slope. At the lower end of the rock glacier the tip of the tongue has slid into steeper terrain causing a landslide-like surface topography. A detailed morphological analysis of Hinteres Langtalkar rock glacier is given by Lieb et al. (2004) and Avian et al. (2005). The surface flow/creep velocity and surface height change of Hinteres Langtalkar rock glacier were examined using photogrammetric and geodetic methods (this chapter). Additionally, the steep frontal slope of the rock glaciers was investigated by terrestrial laser scanning (cp. Avian, 2008).

The morphodynamics of Hinteres Langtalkar rock glacier and especially the temporal development of its tension cracks have been nicely visualized in animated GIFs. Multi-temporal orthophotos were stacked on top of each other and shown in a temporal sequence. See animations on the DVD attached to this document.

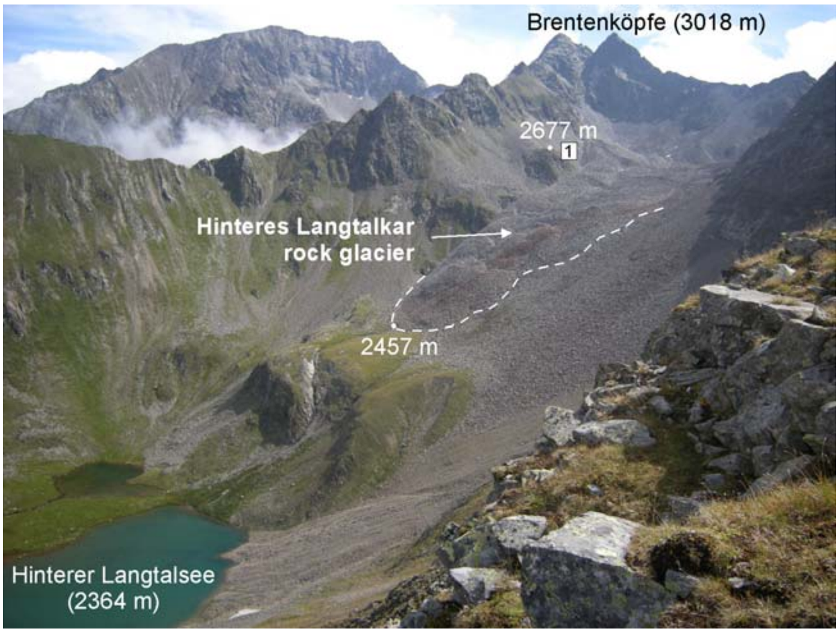

Figure 18: Terrestrial view of Hinteres Langtalkar rock glacier as seen from Hinterseekamp ridge (2580 m). The annual geodetic survey of the rock glacier is carried out from position "1" (2677 m) with a total station. Photograph taken by V. Kaufmann on 22 August 2008.

7.2. Aerial photogrammetry

Aerial photographs of 10 different epochs between 1954 and 2006 were evaluated following the scheme outlined earlier in Section 5.3 (cp. review paper of Kaufmann and Ladstädter, 2009). Dense 3D displacement vector fields and high-resolution digital elevation models were computed providing the basis for detailed geomorphological analysis (for the latter see Avian et al., 2005, and Kellerer-Pirklbauer and Kaufmann, 2007). Morphometric results are not only presented in Kaufmann and Ladstädter (2009), but also in Kaufmann and Ladstädter (2002b, 2003 and 2004b). Large horizontal strain rates of up to $20\text{-}23\times10^{-3}$ a^{-1} were deduced from the photogrammetric measurements. The annual rate of surface lowering due to permafrost melt is rather difficult to estimate since the height measurement accuracy of aerial photogrammetry is limited to the decimeter level in most cases. Significant results in surface height change can only be obtained for multi-temporal stereopairs if the time interval is large enough. Keeping in mind some pre-assumptions, surface lowering due to permafrost degradation/ice melt at Hinteres Langtalkar rock glacier was estimated to be in the range between -1.2 and -5.0 cm/year. The author proposes the application of airborne laser scanning (ALS) for obtaining high-resolution digital elevation models in a future project. Anticipated height accuracies at the centimeter level are feasible (Pfeifer and Mandlburger, 2009).

7.3. Geodetic measurements

In 1998, a geodetic network consisting of more than 10 stable reference points was set up by Kienast and Kaufmann (2004). 38 observation points were stabilized on the rock glacier using brass bolts. The positions of these observation points have since been measured annually using a total station. Figure 19 presents the displacement vectors obtained for the time period 2007-2008. A maximum horizontal flow velocity of 2.38 m/year was measured at point number 23 for the time period 2003-2004. The present status of the geodetic monitoring program can always be retrieved from Kaufmann (2009). An analysis of the mean annual surface flow velocities obtained is presented in Chapter 9.

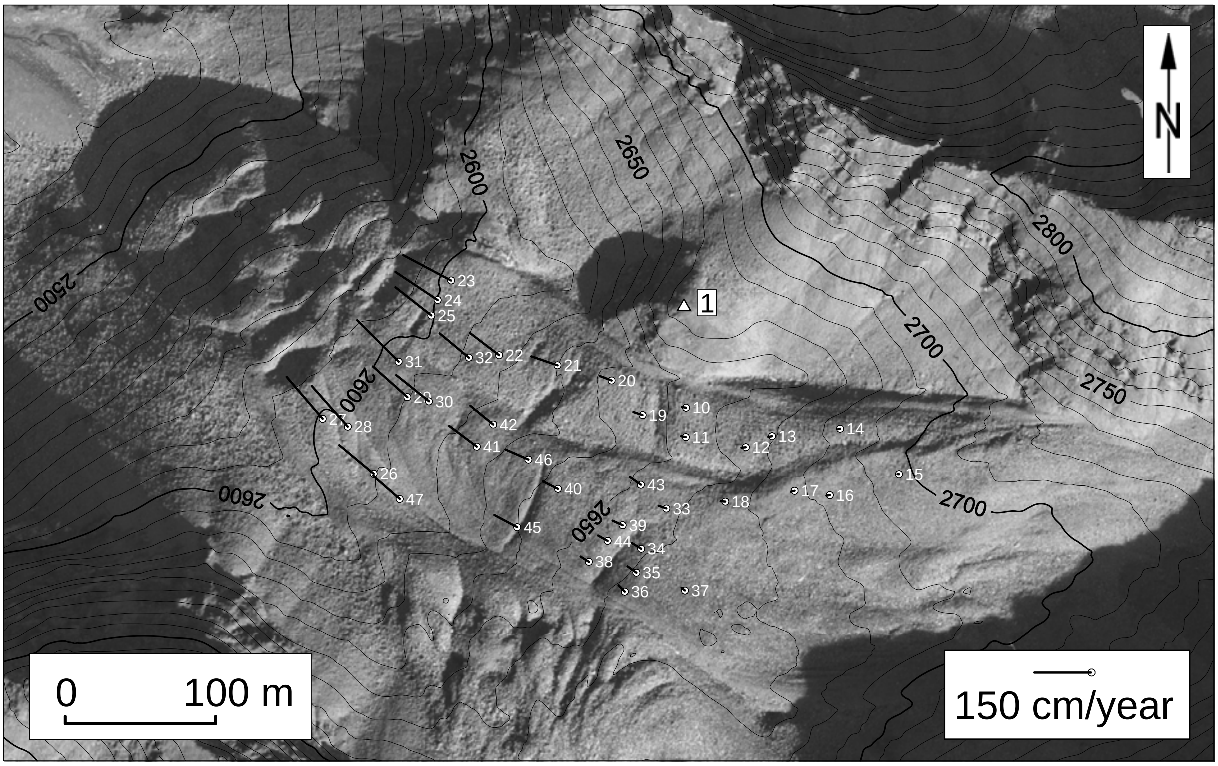

Figure 19: Horizontal movement of the 38 observation points of Hinteres Langtalkar rock glacier for the time period 2007-2008. The position of the total station used is at reference point number 1 marked with a triangle. Orthophoto of 21 September 2006.

8. Weissenkar rock glacier (East Tyrol, Austrian Alps)

8.1. Introduction and geographical setting

Weissenkar rock glacier (46°57'29"N, 12°45'11"E; Schober Mountains, Hohe Tauern Range) is the third rock glacier of the author's monitoring program in the Hohe Tauern Range. The rock glacier is located in a glacially shaped cirque southwest of Gössnitzkees (see GLACIER-Map, 1998, Appendix A13). It is approx. 500 m long and up to 300 m wide and is a good example of the typical viscous flow of creeping permafrost (cp. Figure 20). More information on the geographical setting of the rock glacier can be found in Buchenauer (1990), and Lieb and Krobath (2006). Most interestingly, the movement of Weissenkar rock glacier is retarded by a riegel located in the northwestern end of the rock glacier tongue. Weissenkar rock glacier is at present a relatively slowly creeping rock glacier with mean annual horizontal flow velocities up to 12 cm/year. A monitoring program similar to that of Doesen rock glacier and Hinteres Langtalkar rock glacier was set up in 1997. Furthermore, automatic and continuous measurements of ground surface temperature were also started in the same year to support climate change studies (Kellerer-Pirklbauer et al., 2008).

Figure 20: Terrestrial view of Weissenkar rock glacier. Viewing direction towards southeast. Photograph taken by V. Kaufmann on 25 August 2007.

8.2. Aerial photogrammetry

Large-scale aerial photographs of three different epochs, i.e., 1974, 1998 and 2003, covering the area of interest were taken into consideration. Precise 3D surface displacement vectors and high-resolution multi-temporal DEMs were obtained applying digital photogrammetric methods (Kaufmann et al., 2006). Maximum mean annual horizontal flow velocities of up to 10 cm/year were measured for the time intervals 1974-1998 and 1998-2002. Figure 21 shows the horizontal displacement vectors of a small part of the rock glacier for the time interval 1974-1998. Overall surface height change for the whole rock glacier was estimated at -2 cm/year for the same time period, which is in good agreement with the results obtained for the other two rock glaciers, i.e., Doesen rock glacier and Hinteres Langtalkar rock glacier.

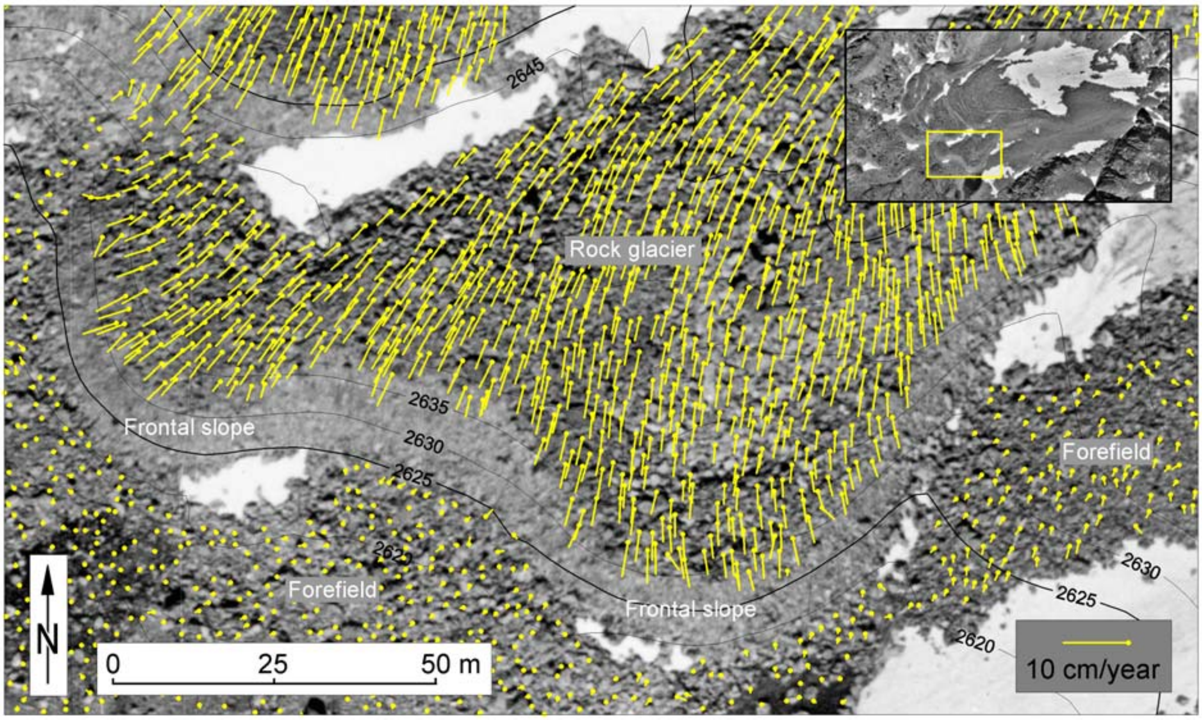

Figure 21: Dense field of horizontal displacement vectors at Weissenkar rock glacier. Vectors were derived from aerial photographs of 1974 and 1998 applying ADVM software.

8.3. Geodetic measurements

Geodetic measurements were commenced in 1997 (Kienast and Kaufmann, 2004). In 2007, the geodetic network consisting of 2 stable reference points was augmented by an additional five points. 18 observation points of the rock glacier surface were fixed with brass bolts on large boulders. Displacement vectors of these points were determined geodetically on a yearly basis, with one exception in 2002 when bad weather made measurements impossible. The highest creep velocities were always measured for the uppermost points, reaching maximum values up to 11.6 cm/year (2001-2003). Compressive flow in the lower part of the rock glacier was proven by geodetically measuring significant uplift of the surface. A comparative analysis of the photogrammetric and geodetic measurements is given in Kaufmann et al. (2006).

9. Impact of atmospheric warming

As already indicated, climate change has an influence on mountain environments. Atmospheric warming is causing glacier melt and permafrost degradation (Haeberli, W. and Maisch, M., 2007; Harris et al., 2008).

Gössnitzkees is a drastic example of on-going glacier melt. Permafrost degradation goes alongside with rock glacier surface lowering due to ice melt and with rock glacier flow/creep speed-up due to more favorite conditions for higher flow/creep rates.

Climatically induced rock glacier surface lowering was estimated at centimeter level based on photogrammetric and geodetic measurements. Since surface height change observed on rock glaciers depends on various parameters, such as topography of bedrock, internal structure, hydrology, etc., appropriate modeling is necessary to separate the climatically induced component from the other ones. Improved geometric observation techniques, such as airborne laser scanning or even highly redundant digital aerial photography, can help to obtain a more reliable estimate concerning permafrost degradation. Mass balance studies will need to be addressed in the future.

Rock glacier speed-up within the past decade has been observed on several rock glaciers in the European Alps. All four rock glaciers with a geodetic observation program (for Inner Hochebenkar rock glacier only photogrammetric measurements are available) match very well with the results obtained elsewhere (Delaloye et al., 2008). Figure 22 summarizes the flow/creep behavior of the three rock glaciers located in the Hohe Tauern Range for the past years. Congruent flow behavior over time can be recognized to a high degree. Detailed correlation analysis with air temperature records from adjacent meteorological stations and in-situ ground surface temperature measurements suggest that there is a positive correlation between temperatures and rock glacier flow/creep velocity (cp. Buck and Kaufmann, 2009, and Kellerer-Pirklbauer et al., 2008). Buck and Kaufmann discovered that the horizontal displacement rates show a fairly clear correlation with variations in mean annual air temperature (MAAT) with a delay of about a year caused by their delayed propagation deeper into the ground. However, the vertical displacement rates seem to react faster to the MAAT.

Measurement records are still too short. In general, process understanding, modeling and, for example, mapping of winter snow cover, need to be improved. In this context the interested reader is referred to Frauenfelder et al. (2008) and also to PERMOS, which is a comprehensive monitoring network of mountain permafrost built up in the Swiss Alps (cp. Vonder Mühll et al., 2008).

As far as remote sensing of rock glaciers is concerned, higher measuring accuracy and a better temporal resolution is needed. However, pluri-annual and decadal photogrammetric analyses provide helpful insight into rock glacier kinematics, especially when historic image data is available (Kääb, 2007; Kaufmann, this volume).

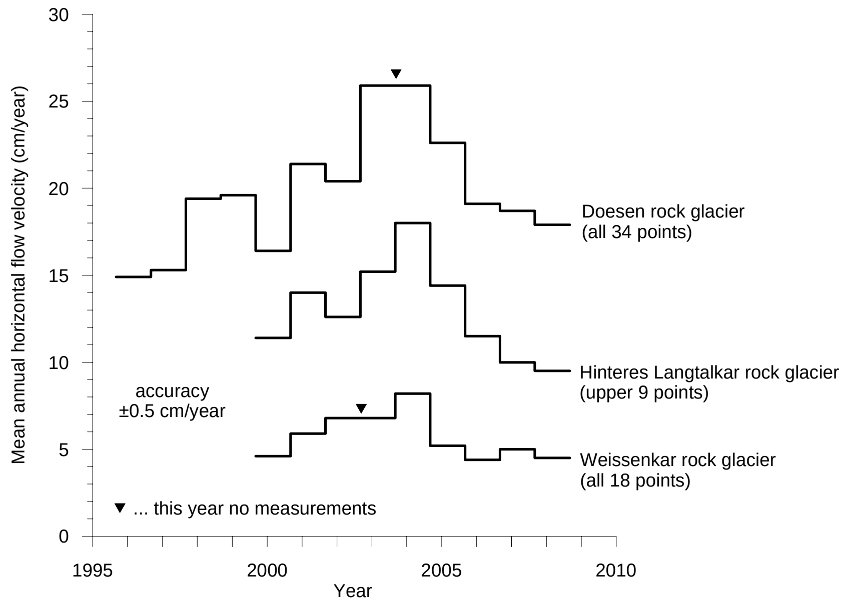

Figure 22: Variation of mean annual horizontal flow velocity of three Austrian rock glaciers in the Hohe Tauern Range.

10. Blaubach landslide (Salzburg, Austrian Alps)

10.1. Introduction and geographical setting

Mass movements, such as landslides, debris flows, mudflows, or rockfalls, are a major threat to infrastructure and life in many parts of the world. Investigations on slope stability and hazard zone mapping have become a matter of concern worldwide during the past two decades (cp. Varnes, 1984). Landslides, for example, are also a common geomorphological hazard in Austria (Embleton-Hamann, 2007). Active landslides need to be studied in detail applying various observation techniques for hazard zone mapping and, eventually, for setting up countermeasures aimed at preventing damage. Knowledge of the landslide topography and its temporal change is indispensable. The kinematic state of a landslide can be observed and monitored by several observation techniques, for example, GPS survey, geodetic survey using a total station, aerial photogrammetry, satellite-based differential SAR interferometry (DInSAR), ground-based radar interferometry, and other methods.

Deformation measurements in natural landscapes have had a long tradition in civil engineering, and a vast amount of literature is available. Hartinger (2001), Antonello et al. (2004), Strozzi et al. (2005) and Chandler et al. (2007) are suggestions for further reading. The concepts of geodetic deformation analysis are outlined for example in Lienhart (2008).

The application of satellite-based positioning using GPS technology has been demonstrated by Hartinger (2001) at the Gradenbach landslide, Carinthia, Austria. At this study site aerial photogrammetry was also applied in order to retrieve displacement vectors using multi-temporal aerial photographs (Brückl et al., 2006). Other studies using photogrammetric methods have been published in, for example, Cunietti et al. (1984), Mora et al. (2003), Walstra et al. (2004) and Chadwick et al. (2005). In this chapter the author wants to transfer his concept of measuring 3D displacement vectors, originally developed for monitoring of rock glaciers, to the landslide example.

The Blaubach landslide (47°13'N, 12°08'E) is located in the upper catchment area of the Blaubach torrent, a tributary to Krimmler Ache, in the western part of Salzburg, Austria. The geomorphological setting of the landslide is described, for example, in Zobl (2001) and Anker (2008). Protective measures along the Blaubach torrent have been installed by the Oberpinzgau regional branch of the Austrian Forest Engineering Service of Torrent and Avalanche Control below the landslide in order to retain eroded material in a controlled manner. Furthermore, a drainage system has been installed in the landslide area for capturing excessive near-surface water. See Figures 23-24. Increased mass transport can be expected after heavy rain events or continuous rainfall over several days. Historical aerial photographs were acquired to quantitatively study relief changes in the past. A geodetic network was installed for documentation of present movements.

Figure 23: Terrestrial view (in flow-line direction) of the lower part of the Blaubach landslide. Vegetation cover is limited due to strong soil erosion, soil creep and slumping. A retaining wall, the uppermost of a cascade, was built as a protective measure in 2003. A subsurface drainage system was installed on the orographic left side of the landslide, in areas with less movement. Photograph taken by V. Kaufmann on 27 September 2008.

10.2. Aerial photogrammetry

Aerial photographs of 12 different epochs between 1953 and 2004 were photogrammetrically evaluated (cp. Kaufmann, 2004b; Kaufmann and Ladstädter, 2007b; Kaufmann, 2008). While at the beginning of the study (2001) an analytical DSR-1 plotter of Kern was used, the photogrammetric processing chain was later on completely ported to the digital photogrammetric workstation ImageStation of Intergraph. The main objective of the photogrammetric work was to document the spatio-temporal evolution of the landslide within the given time period. The creep velocities were computed in two ways: (1) by manual/interactive tracking of individual trees and buildings in the multi-temporal stereomodels, and (2) by measuring 3D displacement vectors applying automatic image matching based on quasi-orthophotos (references). The example of two trees (T1, T2) persistently "riding" on the surface of the landslide, revealed a horizontal movement of 23.90 m and 56.47 m within 51 years, which results in a mean annual creep velocity of 0.47 m/year and 1.11 m/year, respectively. Two buildings (B1, B2) located outside the central part of the landslide were moving downslope at an average rate of 4.4 cm/year. See the location of both the trees and buildings in Figure 24 and Figure 25.

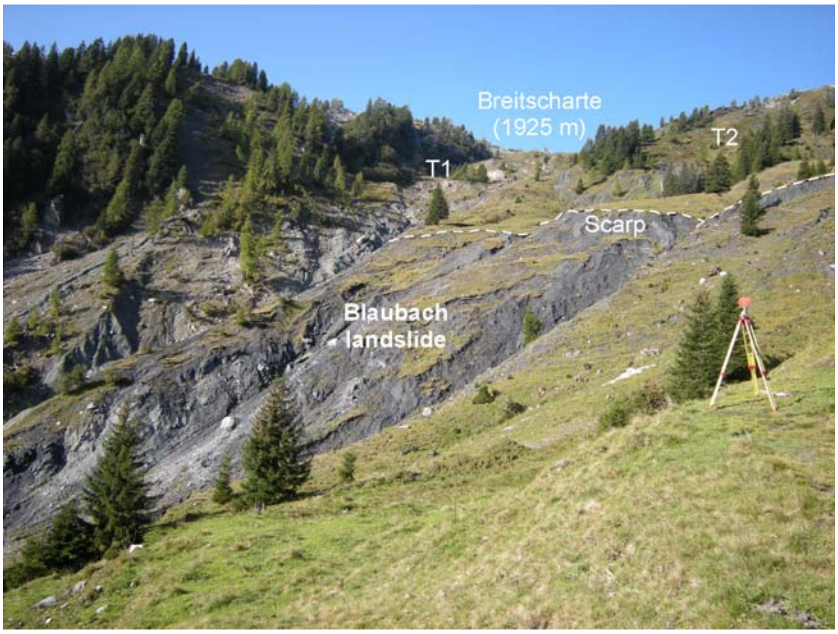

Figure 24: Terrestrial view of the central and upper, orographic right side of the Blaubach landslide. T1 and T2 are two single trees moving downhill on top of the landslide. Below the scarp, indicated by a dashed line, strong denudation takes place (cp. Figure 23). Photograph taken by V. Kaufmann on 28 September 2008.

Dense fields of 3D displacement vectors were automatically obtained by digital image matching based on the concept of quasi-orthophotos. Selected results are shown in the references given in the previous paragraph. Vegetation cover and changing surface textures impede or even prevent successful image matching. This is the reason why further manual editing is needed to exclude gross errors. Wooded areas and bare surfaces reworked by the landslide do not produce any valid solutions. In this context, it is worth mentioning that any surface deformation can be easily detected by viewing at multi-temporal quasi-orthophotos stereoscopically. Parallax differences (= motion parallaxes) induced by the creep process will generate a pseudo-relief. This visible "surface deformation" is generally also measurable in most cases. These quasi-orthophotos can also be used for visualization of morphodynamics and other geomorphological processes. See the computer animations provided on the DVD, Appendix B.

Multi-temporal high-resolution digital elevation models were computed based on classical/interactive photogrammetric mapping and also automatic image matching, the latter being a by-product of the change detection process mentioned earlier. Mass balances were calculated subtracting the multi-temporal DEMs from one another. Erosion rates of up to 12,300 m^3/year were obtained for the area of interest. A thematic visualization of the surface height change in space and time is shown in another computer animation, also included on the DVD.

10.3. Geodetic measurements

A geodetic network consisting of presently four stable reference points (R1-R4) and 41 observation points evenly distributed inside the landslide area was set up in 2001 (see Figure 25) supported by K. Kienast of the Institute of Navigation and Satellite Positioning. This network has since been geodetically surveyed every year in September. Deformation analysis includes stability check of the reference points and subsequent computation of the 3D displacement vectors of the observation points. The results obtained reveal that the movement of the landslide strongly varies from year to year. Temperature and precipitation are identified as the main influencing factors for the kinematic state of the Blaubach landslide. In the observation period 2006-2007, Blaubach landslide showed the least activity with maximum flow/creep velocities of up to 35 cm/year. One year later, however, velocities of up to 148 cm/year were measured, the highest rates ever recorded since 2001 (see Figure 25). The surface topography of the present situation is characterized by active sliding, slumping, soil creep, debris flows, and opening of tension cracks.

10.4. Acknowledgments

The study was funded by the Oberpinzgau regional branch of the Austrian Forest Engineering Service of Torrent and Avalanche Control. The support of Franz Anker is gratefully acknowledged.

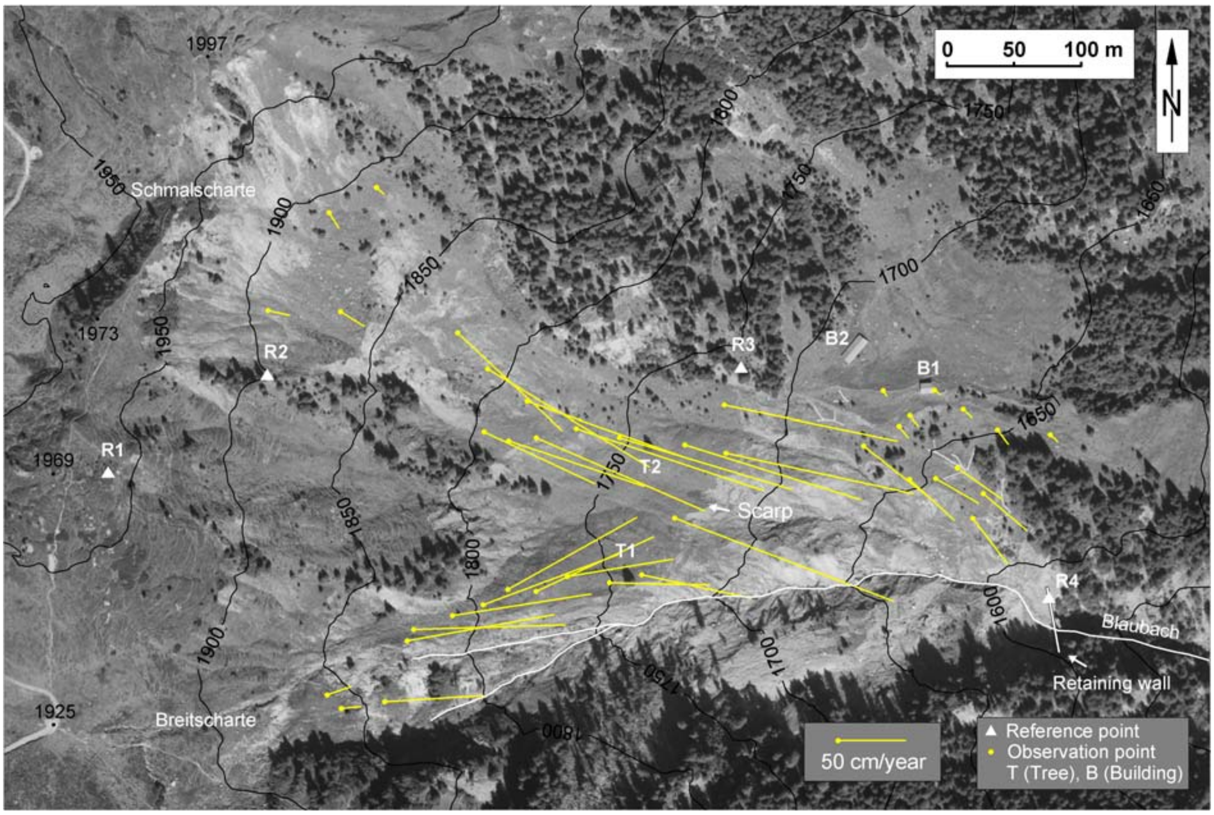

Figure 25: Mean annual horizontal movement of the 41 observation points of Blaubach landslide for the time period 2007-2008. Orthophoto of 6 September 2004.

11. Acknowledgments

The case studies presented in this paper have been elaborated by the author during the past 20 years while working at the Graz University of Technology. Many colleagues, students, volunteers, relatives and friends have participated in and actively supported the research work and field investigations. Unfortunately, it is impossible to thank each individual person within the scope of this publication. However, corresponding acknowledgments have already been provided in each chapter and in the respective papers listed in the references. I particularly wish to thank both my superiors Professor Emeritus Dr. Gerhard Brandstätter and Professor Dr. Mathias Schardt for their liberal attitude at the Institute providing the framework for independent research work. I am indebted to Professor Dr. Franz Leberl, Professor Dr. Manfred Buchroithner and Professor Dr. Robert Kostka, who acted as driving forces on many occasions. I am especially grateful to my colleagues Professor Dr. Gerhard K. Lieb, Dipl.-Ing. Gerhard Kienast and Dr. Richard Ladstädter, who volunteered to work together with me during the past years. Many results obtained and papers published bear their hallmarks. The assistance of Mr. Walter Krämer is gratefully acknowledged. Last but not least I would like to express my appreciation of the kind support from Mrs. Angelika Prohammer, who polished up the English style in a number of papers for me, including this one.

References

References with the name of the first author underlined are attached to this publication in full length. Each of these references has an index number for easy search in the Appendix A.

Albertz, J., 2007: A Look Back – 140 Years of "Photogrammetry", Some Remarks on the History of Photogrammetry. *Photogrammetric Engineering & Remote Sensing*, 73(5), 504-506.

Alexander, D., 1982: Difference between "calanchi" and "biancane" badlands in Italy. In: Bryan, R.B. and Yair, A. (Eds.), *Badland Geomorphology and Piping*, Geo Books, Norwich, 71–87.

Anker, F., 2008: Der Blaubach – Gemeinde Krimml. Wildbach- und Lawinenverbau, *Zeitschrift für Wildbach-, Lawinen-, Erosions- und Steinschlagschutz*, 72(158), in German, 114-120.

Antonello, G., Casagli, N., Farina, P., Leva, D., Nico, G., Sieber, A.J. and Tarchi, D., 2004: Ground-based SAR interferometry for monitoring mass movements. *Landslides*, 1(1), 21-28.

Arenson, L., Hoelzle, M. and Springman, S., 2002: Borehole Deformation Measurements and Internal Structure of Some Rock Glaciers in Switzerland. *Permafrost and Periglacial Processes*, 13(2), 117-135.

Avian, M., Kaufmann, V. und Lieb, G.K., 2005: Recent and Holocene dynamics of a rock glacier system – the example of Langtalkar (Central Alps, Austria). *Norsk Geografisk Tidsskrift – Norwegian Journal of Geography*, 59, 149-156.

Avian, M., Lieb, G.K., Kellerer-Pirklbauer, A. and Bauer, A., 2007: Variations of Pasterze Glacier (Austria) between 1994 and 2006 – Combination of Different Data Sets for Spatial Analysis. *Proceedings, 9th International Symposium on High Mountain Remote Sensing Cartography*, Grazer Schriften der Geographie und Raumforschung, 43, Institute of Geography and Regional Science, University of Graz, 79-88.

Avian, M., Kellerer-Pirklbauer, A. and Bauer, A., 2008: Remote Sensing Data for Monitoring Periglacial Processes in Permafrost Areas: Terrestrial Laser Scanning at the Hinteres Langtalkar Rock Glacier, Austria. In: Kane, D.L. and Hinkel K.M. (Eds.), *Ninth International Conference on Permafrost*, Vol. 1, Institute of Northern Engineering, University of Alaska Fairbanks, 77-82.

AV-Map, 2004: Summit area of Nevado Ojos del Salado 1:35,000. Map extract of "Nevado Ojos Del Salado 1:100,000" published within the framework of the Alpenvereinskartographie by the Deutscher Alpenverein (German Alpine Club) and produced at the Institute of Cartography of the Dresden University of Technology, Germany. **[A3]**

Baltsavias, E.P., 1996: Digital ortho-images – a powerful tool for the extraction of spatial- and geo-information. *ISPRS Journal of Photogrammetry & Remote Sensing*, 51(2), 63-77.

Baltsavias, E.P. and Stallmann, D., 1994: Improvements in matching of SPOT images for DTM generation. *Proceedings, 7th Australasian Remote Sensing Conference*, Melbourne, 314-321.

Bamler, R. and Hartl, Ph., 1998: Synthetic aperture radar interferometry. *Inverse Problems*, 14 (1998), R1-R54, doi:10.1088/0266-5611/14/4/001.

Barsch, D., 1996. *Rockglaciers. Indicators for the Present and Former Geoecology in High Mountain Environments*. Springer Series in Physical Environment, 16, Springer, 331 pages.

Battaglia, S., Leoni, L. and Sartori, F., 2002: Mineralogical and grain size composition of clays developing calanchi and biancane erosional landforms. *Geomorphology*, 49, 153-170.

Bauder, A., Funk, M. and Huss, M., 2007: Ice-volume changes of selected glaciers in the Swiss Alps since the end of the 19th century. *Annals of Glaciology*, 46, 145-149.

Benzinger, R., 1994: Nevado Ojos del Salado (6880 m) – Geomorphometrische Analyse des höchsten Vulkans der Erde. Unpublished Seminar Thesis, Institute of Applied Geodesy and Photogrammetry, Graz University of Technology, in German, 210 pages.

Biard, J., Madani, M. and Jacobsen, K., 2004: Handling of high resolution space images in Z/I ImageStation. IAPRS, Vol. XXXV, Part B1, *Proceedings, 20th Congress of ISPRS*, Istanbul, Turkey, 148-152.

Brückl, E., Brunner, F.K. and Kraus, K., 2006: Kinematics of a deep-seated landslide derived from photogrammetric, GPS and geophysical data. *Engineering Geology*, 88(3-4), 149-159.

Bryan, R.B. and Yair, A., 1982: Perspectives on studies of badland geomorphology. In: Bryan, R.B. and Yair, A. (Eds.), *Badland Geomorphology and Piping*, Geo Books, Norwich, 1–12.

Buchenauer, H.W., 1990: Gletscher- und Blockgletschergeschichte der westlichen Schobergruppe (Osttirol). *Marburger Geographische Schriften*, 117, Philipps-Universität Marburg, in German, 276 pages.

Buchroithner, M.F., 2006: Auf wissenschaftlicher Expedition am Ojos del Salado, dem höchsten Vulkan der Erde. In: Kostka, R. (Ed.), *Aconcagua und die Anden bis zum Wendekreis des Steinbocks*, Weishaupt Verlag, Gnas, Austria, in German, 86-95.

Buck, S. and Kaufmann, V., 2009: The Influence of Air Temperature on the Creep Behaviour of Three Rockglaciers in the Hohe Tauern. *Proceedings, 10th International Symposium on High Mountain Remote Sensing Cartography*, 2008, Kathmandu, Nepal, in print.

Chadwick, J., Dorsch, S., Glenn, N., Thackray, G. and Shilling, K., 2005: Application of multi-temporal high-resolution imagery and GPS in a study of the motion of a canyon rim landslide. *ISPRS Journal of Photogrammetry & Remote Sensing*, 59(4), 212-221.

Chandler, J., Lane, S. and Walstra, J., 2007: Quantifying landform change. In: Fryer, J., Mitchell, H. and Chandler, J. (Eds.), *Applications of 3D Measurement from Images*, Whittles Publishing, UK, 139-170.

Clarke, M.L. and Rendell, H.M., 2006: Process-form relationship in Southern Italian badlands: erosion rates and implications for landform evolution. *Earth Surface Processes and Landforms*, 31, 15-29.

Cronk, S., Fraser, C. and Hanley, H., 2006: Automated metric calibration of colour digital cameras. *The Photogrammetric Record*, 21(116), 355-372.

Csaplovics, E., Kanonier, J. and Sindhuber, A., 1994: High resolution KFA-photography for integration with Geo-Information Systems – a case study of Fertö Tó National Park (Austria, Hungary). In: Vaughan, R. (Ed.), Remote Sensing – From Research to Operational Applications in the New Europe, *Proceedings, 13th EARSeL Symposium*, Dundee, 1993, Springer-Verlag, Budapest, 127-134.

Cunietti, M., Fangi, G., Mussio, L. and Radicioni, F., 1984: Block adjustment and digital model of photogrammetric data in a control problem for the "Ancona '82" landslide. IAPRS, Vol. XXV, Part A3b, *Proceedings, 15th Congress of ISPRS*, Rio de Janeiro, Brazil, 421-432.

Delaloye, R., Lambiel, Ch., Lugon, R., Raetzo, H. and Strozzi, T., 2007: ERS InSAR for Detecting Slope Movement in a Periglacial Mountain Environment (Western Valais Alps, Switzerland). *Proceedings, 9th International Symposium on High Mountain Remote Sensing Cartography*, Grazer Schriften der Geographie und Raumforschung, 43, Institute of Geography and Regional Science, University of Graz, 113-120.

Delaloye, R., Perruchoud, E., Avian, M., Kaufmann, V., Bodin, X., Hausmann, H., Ikeda, A., Kääb, A., Kellerer-Pirklbauer, A., Krainer, K., Lambiel, C., Mihajlovic, D., Staub, B., Roer, I. and Thibert, E., 2008: Recent Interannual Variations of Rock Glacier Creep in the European Alps. In: Kane, D.L. and Hinkel K.M. (Eds.), *Ninth International Conference on Permafrost*, Vol. 1, Institute of Northern Engineering, University of Alaska Fairbanks, 343-348.

de Silva, S.L. and Francis, P.W., 1991: *Volcanoes of the Central Andes*. Springer-Verlag, Berlin, 216 pages.

Ebohon, B. and Schrott, L., 2008: Modeling Mountain Permafrost Distribution: A New Permafrost Map of Austria. In: Kane, D.L. and Hinkel K.M. (Eds.), *Ninth International Conference on Permafrost*, Vol. 1, Institute of Northern Engineering, University of Alaska Fairbanks, 397-402.

Embleton-Hamann, Ch., 2007: Geomorphological Hazards in Austria. In: Kellerer-Pirklbauer, A., Keiler, M., Embleton-Hamann, Ch. and Stötter, J. (Eds.), *Geomorphology for the Future – Conference Proceedings*, Innsbruck University Press, Innsbruck, in German, 33-56.

ESA_ERS, 2009: http://earth.esa.int/ers/ (accessed 31 January 2009).

Farifteh, J. and Soeters, R., 2006: Origin of biancane and calanchi in East Aliano, southern Italy. *Geomorphology*, 77, 142-152.

Fauner, A., Ladstädter, R. and Kaufmann, V., 2008: Geometric Calibration of the Hasselblad H3D Medium Format Camera. IAPRS, Vol. XXXVII, Part B1, *Proceedings, 21th Congress of ISPRS*, Beijing, China, 1077-1082.

Fleischer, K., 1996: Erstellung der Alpenvereinskarte "Nevado Ojos del Salado". Unpublished Diploma Thesis, Institute of Cartography, Dresden University of Technology, in German, 76 pages.

Frauenfelder, R., Schneider, B. and Kääb, A., 2008: Using dynamic modelling to simulate the distribution of rockglaciers. *Geomorphology*, 93(1-2), 130-143.

Fuchs, H., 1986: 3-dimensionale Auswertung von SPOT-Bildern. *Mitteilungen der Forstlichen Bundesversuchsanstalt Wien*, 157, in German, 153-161.

Fuchs, H. and Leberl, F., 1984: Universal Analytical Plotter Software for Photographs with Perspective Geometry (CRISP). *Proceedings, Annual Convention of the American Society of Photogrammetry*, Washington D.C., 774-781.

Gasselt, S., 2007: Landforms indicative of creep of debris and ice. In: *Cold-climate landforms on Mars*. Ph.D. Thesis, Department of Earth Sciences, Freie Universität Berlin, Chapter 3, 21-60.

GLACIER-Map, 1998: Gößnitz- und Hornkees, Schobergruppe – Luftbildkarte 1:10 000. In: Aschenbrenner, J. and Suida, H. (Eds.), *1960-2000 – 40 Jahre glaziologische Forschung; Festschrift für Heinz Slupetzky zum 60. Geburtstag*, Salzburger Geographische Arbeiten, 36, enclosure. **[A13]**

González-Ferrán, O., 1995: *Volcanes de Chile*. Instituto Geográfico Militar, Santiago, Chile, 635 pages.

Gruber, S. and Haeberli, W., 2009: Mountain Permafrost. In: Margesin, R. (Ed.), *Permafrost Soils*, Soil Biology, 16, Springer-Verlag, 33-44.

Gspurning, J., Lazar, R. and Sulzer, W., 2006: Regional Climate and Snow/Glacier Distribution in Southern Upper Atacama (Ojos del Salado) – an integrated statistical, GIS and RS based approach. *Grazer Schriften der Geographie und Raumforschung*, 41, Institute of Geography and Regional Science, University of Graz, Austria, 59-70.

Gudmundsson, G.H., 1994: Converging Glacier Flow – A Case Study: the Unteraarglacier. *Mitteilungen der Versuchsanstalt für Wasserbau, Hydrologie und Glaziologie der ETH Zürich*, 131, in German, 120 pages.

Guerricchio, A. and Melidoro, G., 1982: New views of the origin of badlands in the Plio-Pleistocenic clays of Italy. *Proceedings, IV Congress International Association of Engineering Geology*, Vol. II, New Delhi, 227-238.

Haeberli, W. and Maisch, M., 2007: Klimawandel im Hochgebirge. In: Endlicher, W. and Gerstengarbe, F.-W. (Eds.), *Der Klimawandel – Einblicke, Rückblicke und Ausblicke*, Potsdam-Institut für Klimafolgenforschung e.V., in German, 98-107.

Haeberli, W. and Gruber, S., 2008: Research Challenges for Permafrost in Steep and Cold Terrain: An Alpine Perspective. In: Kane, D.L. and Hinkel K.M. (Eds.), *Ninth International Conference on Permafrost*, Vol. 1, Institute of Northern Engineering, University of Alaska Fairbanks, 597-605.

Haeberli, W. and Gruber, S., 2009: Global Warming and Mountain Permafrost. In: Margesin, R. (Ed.), *Permafrost Soils*, Soil Biology, 16, Springer-Verlag, 205-218.

Haeberli, W. and Patzelt, G., 1982: Permafrostkartierung im Gebiet der Hochebenkar-Blockgletscher, Obergurgl, Ötztaler Alpen. *Zeitschrift für Gletscherkunde und Glazialgeologie*, 18(2), 127-150.

Haeberli, W., Hallet, B., Arenson, L., Elconin, R., Humlum, O., Kääb, A., Kaufmann, V., Ladanyi, B., Matsuoka, N., Springman, S., and Vonder Mühll, D., 2006: Permafrost Creep and Rock Glacier Dynamics. *Permafrost and Periglacial Processes*, 17(3), 189-214.

Haeberli, W., Hoelzle, M., Paul, F. and Zemp, M., 2007: Integrated monitoring of mountain glaciers as key indicators of global climate change: the European Alps. *Annals of Glaciology*, 46, 150-160.

Harris, C., Vonder Mühll, D., Isaksen, K., Haeberli, W., Sollid, J.L., King, L., Holmlund, P., Dramis, F., Guglielmin, M. and Palacios, D., 2003: Warming permafrost in European mountains. *Global and Planetary Change*, 39, 215-225.

Harris, C., Arenson, L.U., Christiansen, H.H., Etzelmüller, B., Frauenfelder, R., Gruber, S., Haeberli, W., Hauck, C., Hölzle, M., Humlum, O., Isaksen, K., Kääb, A., Kern-Lütschg, M.A., Lehning, M., Matsuoka, N., Murton, J.B., Nötzli, J., Phillips, M., Ross, N., Seppälä, M., Springman, S.M. and Vonder Mühll, D., 2008: Permafrost and climate in Europe: Monitoring and modelling thermal, geomorphological and geotechnical responses. *Earth Science Reviews*, 2008, doi: 10.1016/j.earscirev.2008.12.002.

Hartinger, H., 2001: Development of a Continuous Deformation Monitoring System using GPS. Dissertation, Institute of Engineering Geodesy and Measurement Systems, Graz University of Technology, Shaker Verlag GmbH, Aachen, 80 pages.

Hengl, T. and Reuter, H.I., 2009: *Geomorphometry. Concepts, Software, Applications.* Developments in Soil Science, 33, Elsevier, 765 pages.

Höhle, J.K. and Potucková, M., 2005: Automated Quality Control for Orthoimages and DEMs. *Photogrammetric Engineering & Remote Sensing*, 71(1), 81-87.

Hurni, L., Kääb, A. and Häberling, Ch., 2000: Kartographische Darstellung glazialer Phänomene. Zeitliche Entwicklung und heutiger Stand. In: Aschenbrenner, J. and Suida, H. (Eds.), *1960-2000 – 40 Jahre glaziologische Forschung; Festschrift für Heinz Slupetzky zum 60. Geburtstag*, Salzburger Geographische Arbeiten, 36, in German, 23-38.

ISPRS, 2009: http://www.isprs.org/ (accessed 31 January 2009).

Jabobsen, K., 1992: Advantages and disadvantages of different space images for mapping. *International Archives of Photogrammetry and Remote Sensing*, Vol. XXIX, Part B2, Washington D.C., 162-168.

Kääb, A., 1996: Photogrammetrische Analyse zur Früherkennung gletscher- und permafrostbedingter Naturgefahren im Hochgebirge. *Mitteilungen der Versuchsanstalt für Wasserbau, Hydrologie und Glaziologie der ETH Zürich*, 145, in German, 182 pages.

Kääb, A., 2005: Remote Sensing of Mountain Glaciers and Permafrost Creep. *Schriftenreihe Physische Geographie – Glaziologie und Geomorphodynamik*, 48, Geographisches Institut, Universität Zürich, 264 pages.

Kääb, A., 2007: Climate Change Impacts on Rockglaciers. *Ice and Climate: The WCRP/SCAR Climate and Cryosphere Newsletter*, 9, June 2007, 10-11.

Kääb, A., 2008: Remote Sensing of Permafrost-related Problems and Hazards. *Permafrost and Periglacial Processes*, 19(2), 107-136.

Kääb, A., Isakowski, Y., Paul, F., Neumann, A. and Winter, R., 2003: Glaziale und periglaziale Prozesse: Von der statischen zur dynamischen Visualisierung. *Kartographische Nachrichten*, 53(5), 206-212.

Kääb, A. and Weber, M., 2004: Development of Transverse Ridges on Rock Glaciers: Field Measurements and Laboratory Experiments. *Permafrost and Periglacial Processes*, 15(4), 379-391.

Kääb, A. and Reichmuth, T., 2005: Advance mechanisms of rockglaciers. *Permafrost and Periglacial Processes*, 16(2), 187-193.

Kääb, A., Frauenfelder, R. and Roer, I., 2007: On the response of rockglacier creep to surface temperature increase. *Global and Planetary Change*, 56(1-2), 172-187.

Kaufmann, V., 1983: Automatische Punkthöhenbestimmung aus zwei beliebig orientierten Meßaufnahmen durch digitale Off-Line-Stereokorrelation. Unpublished Seminar Thesis, Institute of Applied Geodesy and Photogrammetry, Graz University of Technology, in German, 83 pages.

Kaufmann, V., 1984: Entwicklung und Erprobung eines Verfahrens zur geometrischen Auswertung von digitalen multispektralen Zeilenabtasteraufnahmen und analog/digital-gewandelten Luftbildern. Unpublished Diploma Thesis, Institute of Applied Geodesy and Photogrammetry, Graz University of Technology, in German, 210 pages.

<u>Kaufmann</u>, V., 1996: Der Dösener Blockgletscher – Studienkarten und Bewegungsmessungen. In: Lieb, G.K. (Ed.), Beiträge zur Permafrostforschung in Österreich, *Arbeiten aus dem Institut für Geographie der Karl-Franzens-Universität Graz*, 33, in German, 141-162. **[A17]**

<u>Kaufmann</u>, V., 1998a: Topographic Mapping of The Volcano Nevado Ojos Del Salado using Optical and Microwave Image Data. *Geocarto International*, 13(2), 53-64. **[A2]**

Kaufmann, V., 1998b: Geomorphometric monitoring of active rock glaciers in the Austrian Alps. *Proceedings, 4th International Symposium on High Mountain Remote Sensing Cartography*, Research Report 97:3 Natural Sciences/ Technology, The University of Karlstad, 97-113.

Kaufmann, V., 1998c: Deformation analysis of the Doesen rock glacier (Austria). In: Lewkowicz, A.G. and Allard, M. (Eds.), *Proceedings, 7th International Conference on Permafrost*, Yellowknife, Canada, Collection Nordicana, 551-556.

Kaufmann, V., 2004a: Zur Topographie und Morphodynamik des Blockgletschers Hinteres Langtalkar (Schobergruppe, Nationalpark Hohe Tauern, Österreich, Österreich). *Kartographische Nachrichten*, 54(6), in German, 258-262. **[A21]**

Kaufmann, V., 2004b: Morphometric documentation and computer-based visualization of slope deformation and slope creep of the Blaubach landslide (Salzburg, Austria). *Proceedings, 7th International Symposium on High Mountain Remote Sensing Cartography*, 2002, Bishkek, Kyrgyzstan, Kartographische Bausteine, 28, Institute for Cartography, Dresden University of Technology, 99-107. **[A26]**

Kaufmann, V., 2008: Zur Kinematik der Massenbewegung im Talschluss des Blaubaches, Gemeinde Krimml. Wildbach- und Lawinenverbau, *Zeitschrift für Wildbach-, Lawinen-, Erosions- und Steinschlagschutz*, 72(158), in German, 122-129. **[A28]**

Kaufmann, V., 2009: http://www.geoimaging.tugraz.at/viktor.kaufmann/ (accessed 31 January 2009).

Kaufmann, K.-U. and Buchroithner, M.F., 1994: Herstellung und Anwendungsmöglichkeiten von Satellitenbildkarten durch digitale Kombination von Landsat-TM- und KWR-1000-Daten. *Zeitschrift für Photogrammetrie und Fernerkundung*, 62(4), in German, 133-137.

Kaufmann, V., Mattner, W., Raggam, J., Almer, A. and Schnell, J., 1994: Stereo-Radargrammetric Evaluation of ERS-1 SAR Images: A Case Study in Southern Italy. *Proceedings, 2nd ERS-1 Symposium on Space at the Service of our Environment,* 1993, Hamburg, Germany, ESA SP-361, Vol. II, 1211-1216. **[A5]**

Kaufmann, V. and Fastner, U., 1995: Some experiments on relief mapping from space using microwave and optical image data: Looking at the Badlands in Southern Italy. In: Vaughan, R. and Askne, J. (Eds.), Topography from Space, *EARSeL Advances in Remote Sensing*, 4(2), 130-138. **[A6]**

Kaufmann, V. and Lieb, G.K., 1997: Environmental study on a badland area in Southern Italy. In: Spiteri, A. (Ed.), Remote Sensing ’96: Integrated Applications for Risk Assessment and Disaster Prevention for the Mediterranean, *Proceedings, 16th EARSeL Symposium*, Malta, 1996, A.A. Balkema, Rotterdam, 127-134. **[A4]**

Kaufmann, V. and Sulzer, W., 1997: Über die Nutzungsmöglichkeit hochauflösender amerikanischer Spionage-Satellitenbilder (1960-1972). *Österr. Z. f. Vermessung u. Geoinformation*, 85(3), in German, 166-174. **[A7]**

Kaufmann, V. and Heiland, R., 1998: Zur Morphometrie des Dösener Blockgletschers (Nationalpark Hohe Tauern, Österreich). In: Kriz, K. (Ed.), Hochgebirgskartographie/ Silvretta '98 – High Mountain Cartography, *Wiener Schriften zur Geographie und Kartographie*, 11, in German, 102-114.

Kaufmann, V. and Plösch, R., 2000: Mapping and visualization of the retreat of two cirque glaciers in the Austrian Hohe Tauern National Park. *International Archives of Photogrammetry and Remote Sensing*, Vol. XXXIII, Part B4, Amsterdam, 446-453. **[A8]**

Kaufmann, V. and Plösch, R., 2001: Reconstruction and visualization of the retreat of two cirque glaciers in the Austrian Alps since 1850 – From static maps towards dynamic computer animation. In: Buchroithner, M. (Ed.), High Mountain Cartography, Proceedings, Second International Symposium of the Commission on Mountain Cartography of the International Cartographic Association, *Kartographische Bausteine*, 18, Dresden University of Technology, 239-253.

Kaufmann, V. and Ladstädter, R., 2002a: Spatio-temporal analysis of the dynamic behaviour of the Hochebenkar rock glaciers (Oetztal Alps, Austria) by means of digital photogrammetric methods. *Proceedings, 6th International Symposium on High Mountain Remote Sensing Cartography*, Grazer Schriften der Geographie und Raumforschung, 37, Institute of Geography and Regional Science, University of Graz, 119-139. **[A14]**

Kaufmann, V. and Ladstädter, R., 2002b: Monitoring of active rock glaciers by means of digital photogrammetry. *Proceedings, ISPRS Commission III Symposium "Photogrammetric Computer Vision"*, Graz, Austria, IAPRS, Vol. 34, Part 3B, 108-111. **[A15]**

Kaufmann, V. and Ladstädter, R., 2003: Quantitative analysis of rock glacier creep by means of digital photogrammetry using multi-temporal aerial photographs: two case studies in the Austrian Alps. In: Phillips, M., Springman, S.M. and Arenson, L.U. (Eds.), Permafrost, *Proceedings, 8th International Conference on Permafrost*, Vol. 1, Zurich, Switzerland, Swets & Zeitlinger Publishers, 525-530. **[A23]**

Kaufmann, V. and Ladstädter, R., 2004a: Documentation of the retreat of a small debris-covered cirque glacier (Goessnitzkees, Austrian Alps) by means of terrestrial photogrammetry. *Proceedings, 4th ICA Mountain Cartography Workshop*, Vall de Núria, Catalonia, Spain, Monografies tècniques 8, Institut Cartogràfic de Catalunya, Barcelona, 65-76.

Kaufmann, V. and Ladstädter, R., 2004b: Documentation of the Movement of the Hinteres Langtalkar Rock Glacier. IAPRS, Vol. XXXV, Part B7, *Proceedings, 20th Congress of ISPRS*, Istanbul, Turkey, 893-898. **[A22]**

Kaufmann, V. and Ladstädter, R., 2005: Elimination of color fringes in digital photographs caused by lateral chromatic aberration. *Proceedings, XX International Symposium CIPA 2005*, Turin, Italy, Vol. 1, 403-408. **[A11]**

Kaufmann, V., Kenyi, L.W. and Avian, M., 2005: Messung der Fließgeschwindigkeit von Gletschern mittels satellitengestützter Radar-Interferometrie in der Schobergruppe (Nationalpark Hohe Tauern, Kärnten). Unpublished final report submitted to the Carinthian National Park Fonds, 59 pages.

Kaufmann, V., Ladstädter, R. and Lieb, G.K., 2006: Quantitative assessment of the creep process of Weissenkar rock glacier (Central Alps, Austria). *Proceedings, 8th International Symposium on High Mountain Remote Sensing Cartography*, Grazer Schriften der Geographie und Raumforschung, 41, Institute of Geography and Regional Science, University of Graz, 77-86. [**A25]**

Kaufmann, V., Ladstädter, R. and Kienast, G., 2007: 10 years of monitoring of the Doesen rock glacier (Ankogel group, Austria) – A review of the research activities for the time period 1995-2005. In: Petrovič, D. (Ed.), *Proceedings, 5th Mountain Cartography Workshop*, Bohinj, Slovenia, 129-144. **[A18]**

Kaufmann, V. and Ladstädter, R., 2007a: Mapping of the 3D surface motion field of Doesen rock glacier (Ankogel group, Austria) and its spatio-temporal change (1954-1998) by means of digital photogrammetry. *Proceedings, 9th International Symposium on High Mountain Remote Sensing Cartography*, Grazer Schriften der Geographie und Raumforschung, 43, Institute of Geography and Regional Science, University of Graz, 127-144. **[A19]**

Kaufmann, V. and Ladstädter R., 2007b: Photogrammetrische und geodätische Dokumentation der Hangrutschung Blaubachgraben (Gemeinde Krimml, Salzburg) für den Zeitraum 1953 bis 2006. In: Brunner, F.K. (Ed.), *Ingenieurvermessung 07 – Beiträge zum 15. Internationalen Ingenieurvermessungskurs Graz, 2007*, Herbert Wichmann Verlag, 317-322. **[A27]**

Kaufmann, V. and Ladstädter, R., 2008a: Documentation of the Retreat of Gössnitzkees and Hornkees Glaciers (Hohe Tauern Range, Austria) for the Time Period 1997-2006 by Means of Aerial Photogrammetry. *Proceedings, 6th ICA Mountain Cartography Workshop "Mountain Mapping and Visualisation"*, Lenk, Switzerland, 115-123. **[A9]**

Kaufmann, V. and Ladstädter, R., 2008b: Application of Terrestrial Photogrammetry for Glacier Monitoring in Alpine Environments. IAPRS, Vol. XXXVII, Part B8, *Proceedings, 21st Congress of ISPRS*, Beijing, China, 813-818. **[A10]**

Kaufmann, V. and Ladstädter, R., 2009: Documentation and visualization of the morphodynamics of Hinteres Langtalkar rock glacier (Hohe Tauern range, Austrian Alps) based on aerial photographs (1954-2006) and geodetic measurements (1999-2007). *Proceedings, 10th International Symposium on High Mountain Remote Sensing Cartography*, 2008, Kathmandu, Nepal, in print. **[A24]**

Kellerer-Pirklbauer, A. and Kaufmann, V., 2007: Paraglacial Talus Slope Instability in Recently Deglaciated Cirques (Schober Group, Austria). *Proceedings, 9th International Symposium on High Mountain Remote*

Sensing Cartography, Grazer Schriften der Geographie und Raumforschung, 43, Institute of Geography and Regional Science, University of Graz, 121-130.

Kellerer-Pirklbauer, A., Kaufmann, V., Krobath, M., Lieb, G.K. and Avian, M., 2008: 10 Years of Monitoring the Rock Glacier Kinematic and Surface Temperature at Weissenkar Rock Glacier, Austria (1997-2007). *Geophysical Research Abstracts*, Vol. 10, EGU2008-A-02061, 2 pages.

Kenyi, L.W. and Kaufmann, V., 2003a: Estimation of Rock Glacier Surface Deformation Using SAR Interferometry Data. *IEEE Transactions on Geoscience and Remote Sensing*, 41(6), 1512-1515. **[A20]**

Kenyi, L.W. and Kaufmann, V., 2003b: Measuring rock glacier surface deformation using SAR interferometry. Permafrost. In: Phillips, M., Springman, S.M. and Arenson, L.U. (Eds.), Permafrost, *Proceedings, 8th International Conference on Permafrost*, Vol. 1, Zurich, Switzerland, Swets & Zeitlinger Publishers, 537-541.

Kienast, G. and Kaufmann, V., 2004: Geodetic measurements on glaciers and rock glaciers in the Hohe Tauern National Park (Austria). *Proceedings, 4th ICA Mountain Cartography Workshop*, Vall de Núria, Catalonia, Spain, Monografies tècniques 8, Institut Cartogràfic de Catalunya, Barcelona, 101-108. **[A12]**

Klostius, W., Kostka, R. and Sulzer, W., 1994: Das KFA-3000 Bild als kostengünstige Datenquelle bei Aufgaben der regionalen Planung. *Österr. Z. f. Vermessung & Geoinformation*, 82(3), in German, 213-218.

Konecny, G., 1995: Current status and future possibilities for topographic mapping from space. In: Vaughan, R. and Askne, J. (Eds.), Topography from Space, *EARSeL Advances in Remote Sensing*, 4(2), 1-18.

Konecny, G. and Lehmann, G., 1984: *Photogrammetrie*. Walter de Gruyter, Berlin, in German, 392 pages.

Konecny, G., 2004: Mapping from space. In: *Commemorative volume for the 60th birthday of Prof. Dr. Armin Grün*, Institute of Geodesy and Photogrammetry, ETH Zurich, 159-161.

Konecny, G., Lohmann, P., Engel, H. and Kruck, E., 1987: Evaluation of SPOT Imagery on Analytical Photogrammetric Instruments. *Photogrammetric Engineering & Remote Sensing*, 53(9), 1223-1230.

Kostka, R. (Ed.), 1987: Die erderkundende Weltraumphotographie und ihre Anwendung in der Gebirgskartographie, *Mitteilungen der Geodätischen Institute der Technischen Universität Graz*, 57, in German, 217 pages.

Kostka, R. and Sharov, A., 1993: An Employment of Russian Spaceborne Photographic Imagery for Urban Mapping: Metric Aspects. *Proceedings, 16th Urban Data Management Symposium*, Vienna, 104-112.

Krainer, K. and Mostler, W., 2001: Der aktive Blockgletscher im Hinteren Langtalkar, Gößnitztal (Schobergruppe, Nationalpark Hohe Tauern, Österreich). *Wissenschaftliche Mitteilungen aus dem Nationalpark Hohe Tauern*, 6, in German, 139-168.

Krainer, K. and Mostler, W., 2006: Flow velocities of active rock glaciers in the Austrian Alps. *Geografiska Annaler*, 88 A (4), 267-280.

Krämer, J. and Illhardt, E., 1990: Nutzung hochauflösender kosmischer Photoaufnahmen der Kamera KFA-1000 für die verkürzte Aktualisierung von Karten im Maßstab 1:25 000. *Vermessungstechnik*, 38(1), in German, 55-59.

Kraus, K. and Sindhuber, A., 1996: Das Potential russischer Weltraumphotographien für verschiedene Anwendungen. *Österr. Z. f. Vermessung & Geoinformation*, 84(1), in German, 17-21.

Krupnik, A. and Schenk, T., 1997: Experiments with matching in the object space for aerotriangulation. *ISPRS Journal of Photogrammetry & Remote Sensing*, 52(4), 160-168.

Krysiecki, J.-M., Bodin, X. and Schoeneich, P., 2008: Collapse of the Bérard Rock Glacier (Southern French Alps). In: Kane, D.L. and Hinkel K.M. (Eds.), *Ninth International Conference on Permafrost*, Extended Abstracts, Institute of Northern Engineering, University of Alaska Fairbanks, 1505-1510.

Ladanyi, B., 2003: Rheology of ice/rock systems and interfaces. In: Phillips, M., Springman, S.M. and Arenson, L.U. (Eds.), Permafrost, *Proceedings, 8th International Conference on Permafrost*, Vol. 1, Zurich, Switzerland, Swets & Zeitlinger Publishers, 621-626.

Ladstädter, R. and Kaufmann, V., 2004: Change detection of a mountain slope by means of ground-based photogrammetry: A case study in the Austrian Alps. *Proceedings, 4th ICA Mountain Cartography Workshop*, Vall de Núria, Catalonia, Spain, Monografies tècniques 8, Institut Cartogràfic de Catalunya, Barcelona, 77-88.

Ladstädter, R. and Kaufmann, V., 2005: Terrestrisch-photogrammetrische Dokumentation des Blockgletschers im Äußeren Hochebenkar. In: Chesi, G. and Weinold, Th. (Eds.), *Internationale geodätische Woche Obergurgl 2005*, Herbert Wichmann Verlag, Heidelberg, in German, 92-101. **[A16]**

Lambiel, Ch., Delaloye, R., Strozzi, T., Lugon, R. and Raetzo, H., 2008: ERS InSAR for Assessing Rock Glacier Activity. In: Kane, D.L. and Hinkel K.M. (Eds.), *Ninth International Conference on Permafrost*, Vol. 1, Institute of Northern Engineering, University of Alaska Fairbanks, 1019-1024.

Lambrecht, A. and Kuhn, M., 2007: Glacier changes in the Austrian Alps during the last three decades, derived from the new Austrian glacier inventory. *Annals of Glaciology*, 46, 177-184.

Lang, H. and Lieb, G.K., 1993: *Die Gletscher Kärntens*. Verlag des Naturwissenschaftlichen Vereins für Kärnten, Klagenfurt, in German, 184 pages.

Leberl, F., 2001: ISPRS Commission III 'Towards Photogrammetric Computer Vision'. *ISPRS Highlights*, 6(2), GITC B.V., Lemmer, The Netherlands, 12-13.

LFC-Map, 1987: Kathmandu Valley 1:100,000. In: Kostka, R. (Ed.), *Die erderkundende Weltraumphotographie und ihre Anwendung in der Gebirgskartographie*, Mitteilungen der Geodätischen Institute der Technischen Universität Graz, 57, enclosure. **[A1]**

Li, Z., Liu, G. and Ding, X., 2006: Exploring the generation of digital elevation models from same-side ERS SAR images: topographic and temporal effects. *The Photogrammetric Record*, 21(114), 124-140.

Lieb, G.K., 1987: Die Gletscher und Blockgletscher im Kärntner Teil der Schobergruppe und ihre Entwicklung seit dem Spätglazial. Unpublished Doctoral Thesis, University of Graz, in German, 286 pages.

Lieb, G.K., 1996: Permafrost und Blockgletscher in den östlichen österreichischen Alpen. In: Lieb, G.K. (Ed.), Beiträge zur Permafrostforschung in Österreich, *Arbeiten aus dem Institut für Geographie der Karl-Franzens-Universität Graz*, 33, in German, 9-125.

Lieb, G.K., 1998: High-mountain permafrost in the Austrian Alps (Europe). In: Lewkowicz, A.G. and Allard, M. (Eds.), *Proceedings, 7th International Conference on Permafrost*, Yellowknife, Canada, Collection Nordicana, 663-668.

Lieb, G.K., 2000: Die Flächenänderungen von Gössnitz- und Hornkees (Schobergruppe, Hohe Tauern) von 1850 bis 1997. In: Aschenbrenner, J. and Suida, H. (Eds.), *1960-2000 – 40 Jahre glaziologische Forschung; Festschrift für Heinz Slupetzky zum 60. Geburtstag*, Salzburger Geographische Arbeiten, 36, in German, 83-96.

Lieb, G.K. and Kaufmann, V., 1985: Vier Jahre Gletschermessung in der Schobergruppe. *Kärntner Naturschutzblätter*, 24, in German, 123-135.

Lieb, G.K., Kaufmann, V. und Avian, M., 2004: Das Hintere Langtalkar (Schobergruppe, Nationalpark Hohe Tauern) – ein Beispiel für die komplexe Morphodynamik in der Hochgebirgsstufe der Zentralalpen. *Mitteilungen der Österreichischen Geographischen Gesellschaft*, 146, in German, 147-164.

Lieb, G.K. and Krobath, M., 2006: Die Schobergruppe, ein stilles Kleinod der Hohen Tauern. In: Theil, W. (Ed.), Berg 2006, *Alpenvereinsjahrbuch*, 130, in German, 272-283.

Lienhart, W., 2008: Geodätische Deformationsanalyse und Structural Health Monitoring: Chancen und Herausforderungen für die Geodäsie. In: Hofmann-Wellenhof, B., Friedrich, K. and Wallner, W. (Eds.), *Universalgeodäsie in Graz: Festschrift*, Verlag der Technischen Universität Graz, in German, 128-139.

Lu, Zh., Kwoun, O. and Rykhus, R., 2007: Interferometric Synthetic Aperture Radar (InSAR): Its Past, Present and Future. *Photogrammetric Engineering & Remote Sensing*, 73(3), 217-221.

Luhmann, Th., Hastedt, H. and Tecklenburg, W., 2006: Modelling of chromatic aberration for high precision photogrammetry. IAPRS, Vol. XXXVI, Part B5, *Proceedings, ISPRS Commission V Symposium*, Dresden, Germany, 173-178.

Madsen, S.N. and Zebker, H.A., 1998: Imaging Radar Interferometry. In: Ryerson, R.A. (Ed.), *Manual of Remote Sensing*, Vol. 2, Principles and Applications of Imaging Radar, John Wiley & Sons, Inc., 359-380.

Mora, P., Baldi, P., Casula, G., Fabris, M., Ghirotti, M., Mazzini, E. and Pesci, A., 2003: Global Positioning Systems and digital photogrammetry for the monitoring of mass movements: applications to the Ca' di Malta landslide (northern Apennines, Italy). *Engineering Geology*, 68(1-2), 103-121.

MountainCarto, 2009: http://www.mountaincartography.org/ (accessed 31 January 2009).

Nagler, T., Mayer, C. and Rott, H., 2002a: Feasibility of DINSAR for mapping complex motion fields of alpine ice- and rock glaciers. *Proceedings, 3rd International Symposium on Retrieval of Bio- and Geophysical Parameters from SAR Data for Land Applications*, Sheffield, U.K., ESA-SP475, 377-382.

Nagler, T., Rott, H. and Kamelger, A., 2002b: Analysis of Landslides in Alpine Areas by Means of SAR Interferometry. *Proceedings, International Geoscience and Remote Sensing Symposium (IGARSS '02)*, Toronto, Canada, IEEE CD-ROM Cat.No. 02CH37380C, 3 pages.

NASA-JSC, 2009: http://eol.jsc.nasa.gov/ (accessed 31 January 2009).

Norvelle, F.R., 1996: Using Iterative Orthophoto Refinements to Generate and Correct Digital Elevation Models (DEM's). In: Greve, C. (Ed.), *Digital Photogrammetry: An Addendum to the Manual of Photogrammetry*. American Society for Photogrammetry and Remote Sensing, Bethesda, Maryland, 151-155.

Oerlemans, J., 2001: *Glaciers and Climate Change*. Swets & Zeitlinger BV, Lisse, 148 pages.

Patzelt, G., Stötter, J., Nicolussi, K. and Wastl, M., 2007: Indicators of Past and Present Climate Changes: Excursion from Obergurgl to Gurgler Ferner. In: Kellerer-Pirklbauer, A., Keiler, M., Embleton-Hamann, Ch. and Stötter, J. (Eds.), *Geomorphology for the Future – Conference Proceedings*, Innsbruck University Press, Innsbruck, in German, 13-22.

Petrie, G. and Toth, C.K., 2009: Terrestrial Laser Scanners. In: Shan, J. and Toth, C.K. (Eds.), *Topographic laser ranging and scanning: principles and processing*, CRC Press, Taylor & Francis Group, 87-127.

Pfeifer, N. and Mandlburger, G., 2009: LiDAR Data Filtering and DTM Generation. In: Shan, J. and Toth, C.K. (Eds.), *Topographic laser ranging and scanning: principles and processing*, CRC Press, Taylor & Francis Group, 307-333.

Pillewizer, W., 1957: Untersuchungen an Blockströmen der Ötztaler Alpen. In: Geomorphologische Abhandlungen, *Abhandlungen des Geographischen Instituts der freien Universität Berlin*, 5, in German, 37-50.

Poli, D., Li, Zh. and Gruen, A., 2004: SPOT-5/HRS stereo images orientation and automated DSM generation. IAPRS, Vol. XXXV, Part B1, *Proceedings, 20th Congress of ISPRS*, Istanbul, Turkey, 421-432.

Raggam, J., 1984: Radar Stereo Model Set-up on the Analytical Plotter Kern DSR-1. *Proceedings of ISPRS*, Rio de Janeiro, 25(3B), Comm. III, 893-902.

Raggam, H., Franke, M. and Gutjahr, K., 2005: Surface Model Extraction from High Resolution Stereo Data over Alpine Terrain. In: Oluić, M. (Ed.), *Proceedings, 24th EARSeL Symposium*, 2004, Dubrovnik, Croatia, Millpress Rotterdam, 411-420.

Remondino, F. and Fraser, C., 2006: Digital camera calibration methods: considerations and comparisons. IAPRS, Vol. XXXVI, Part B5, *Proceedings, ISPRS Commission V Symposium*, Dresden, Germany, 266-272.

Riess, A., Albertz, J., Söllner, R. and Tauch, R., 1993: Neue hochauflösende Satellitenbilddaten aus Rußland. *Zeitschrift für Photogrammetrie und Fernerkundung*, 61(1), in German, 42-46.

Rignot, E., Hallet, B. and Fountain, A., 2002: Rock glacier surface motion in Beacon Valley, Antarctica, from synthetic-aperture radar interferometry. *Geophysical Research Letters*, 29(12), doi:10.1029/2001GL013494, 4 pages.

Rinner, K., Burkhardt, R. et al., 1972: Gletscherphotogrammetrie. In: Kneissl, M. (Ed.), Handbuch der Vermessungskunde, Photogrammetrie, Band III a/2, in German, J.B. Metzlersche Verlagsbuchhandlung, Stuttgart, 1428-1470.

Roer, I., Haeberli, W., Avian, M., Kaufmann, V., Delaloye, R., Lambiel, C. and Kääb, A., 2008: Observations and Considerations on Destabilizing Active Rock Glaciers in the European Alps. In: Kane, D.L. and Hinkel K.M. (Eds.), *Ninth International Conference on Permafrost*, Vol. 2, Institute of Northern Engineering, University of Alaska Fairbanks, 1505-1510.

Rott, H. and Siegl, A., 1999: Analysis of Mass Movements in Alpine Terrain by Means of SAR Interferometry. *Proceedings of IGARSS '99*, Hamburg, Germany, Vol. 4, 1933-1936.

Rott, H., Nagler, T., Rocca, F., Prati, C., Mazzotti, A., Keusen, H., Liener, S. and Tarchi, D., 2003: InSAR techniques and applications for monitoring landslides and subsidence. In: Benes, Th. (Ed.), *Proceedings, 22nd EARSeL Symposium*, 2003, Prague, Czech Republic, Millpress Rotterdam, 25-31.

Schenk, T., Li, J.-Ch. and Toth, Ch., 1990: Hierarchical approach to reconstruct surfaces by using iteratively rectified imagery. *Proceedings, ISPRS Commission V Symposium "Close-Range Photogrammetry Meets Machine Vision"*, Zurich, Switzerland, IAPRS, Vol. 28, Part 5/1, SPIE Volume 1395(1), 108-111.

Schneider, B. and Schneider, H., 2001: Zur 60jährigen Messreihe der kurzfristigen Geschwindigkeitsschwankungen am Blockgletscher im Äusseren Hochebenkar, Ötztaler Alpen, Tirol. *Zeitschrift für Gletscherkunde und Glazialgeologie*, 37(1), in German, 1-33.

Sirkiä, O. and Laiho, A., 1989: An investigation of the geometric properties of the Soviet KFA-1000 space images. *The Photogrammetric Journal of Finnland*, 11(2), 74-83.

Strozzi, T., Kääb, A. and Frauenfelder, R., 2004: Detecting and quantifying mountain permafrost creep from in situ inventory, space-borne radar interferometry and airborne digital photogrammetry. *International Journal of Remote Sensing*, 25(15), 2919-2931.

Strozzi, T., Farina, P., Corsini, A., Ambrosini, C., Thüring, M., Zilger, J., Wiesmann, A., Wegmüller, U. and Werner, C., 2005: Survey and monitoring of landslide displacements by means of L-band satellite SAR interferometry. *Landslides*, 2(3), 193-201.

Sulzer, W., 1994: Geomorphologic Mapping of the Volcano Nevado Ojos del Salado using Optical and Microwave Image Data. *Proceedings, 3rd International Symposium on High-Mountain Remote Sensing Cartography*, IIACE, Mendoza, Argentina, 38-46.

Toutin, Th., 1995: Generating DEM from Stereo Images with a Photogrammetric Approach: Examples with VIR and SAR Data. In: Vaughan, R. and Askne, J. (Eds.), Topography from Space, *EARSeL Advances in Remote Sensing*, 4(2), 110-117.

Toutin, Th. and Gray, L., 2000: State-of-the-art of elevation extraction from satellite SAR data. *ISPRS Journal of Photogrammetry & Remote Sensing*, 55, 13-33.

Trinder, J.C., Donnelly, B.E, and Keong, K.L., 1988: SPOT Mapping Software for Wild Aviolyt BC2 Analytical Plotter. *Proceedings, IGARSS '88 Symposium*, Edinburgh, Scotland, 1801-1806.

Varnes, D.J., 1984: Landslide hazard zonation: a review of principles and practice. Pubished by UNESCO, ISBN 92-3-101895-7, 63 pages.

Verstappen, H.Th., 1983: Geomorphology of the Agri valley, southern Italy. *ITC Journal*, 4, 291-301.

Vietoris, L., 1972: Über den Blockgletscher des Äußeren Hochebenkars. *Zeitschrift für Gletscherkunde und Glazialgeologie*, 8(1-2), in German, 169-188.

Vollmer, M., 1999: *Kriechen alpinen Permafrostes: Grundlagen zur digitalen photogrammetrischen Bewegungsmessung*. Unpublished Diploma Thesis, Institute of Geography, University of Zurich, in German, 69 pages.

Vonder Mühll, D.S., Noetzli, J. and Roer, I., 2008: PERMOS – A Comprehensive Monitoring Network of Mountain Permafrost in the Swiss Alps. In: Kane, D.L. and Hinkel K.M. (Eds.), *Ninth International Conference on Permafrost*, Vol. 2, Institute of Northern Engineering, University of Alaska Fairbanks, 1869-1874.

Walstra, J., Chandler, J.H., Dixon, N. and Dijkstra, T.A., 2004: Time for change – quantifying landslide evolution using historical photographs and modern photogrammetric methods. IAPRS, Vol. XXXV, Part B4, *Proceedings, 20th Congress of ISPRS*, Istanbul, Turkey, 475-480.

Wang, Z. and Li, S., 1999: Detection of Winter Frost Heaving of the Active Layer of Arctic Permafrost Permafrost Using SAR Differential Interferograms. *Proceedings, International Geoscience and Remote Sensing Symposium (IGARSS '99)*, Vol. 4, Hamburg, Germany, 1946-1948.

Wangensteen, B., Tønsberg, O.M., Kääb, A., Eiken, T. and Hagen, J.O., 2006: Surface elevation change and high resolution surface velocities for advancing outlets of Jostedalsbreen. *Geografiska Annaler*, 88 A (1), 55-74.

Wikipedia, 2009: http://en.wikipedia.org/ (accessed 31 January 2009).

Würländer, R. and Eder, K., 1998: Leistungsfähigkeit aktueller photogrammetrischer Auswertemethoden zum Aufbau eines digitalen Gletscherkatasters. *Zeitschrift für Gletscherkunde und Glazialgeologie*, 34, 167-185.

Yeu, B.-M., Lee, Y.-W., Koh, L.-W. and Cho, B.-W., 2000: An experimental results on the refinement of DEMs using iteratively generated ortho-image from SPOT stereopairs. *International Archives of Photogrammetry and Remote Sensing*, Vol. XXXIII, Part B4, Amsterdam, 551-558.

Zobl, F., 2001: Abschätzung der Hangstabilitätsverhältnisse im Bereich des Einzugsgebietes der Krimmler Ache/Blaubach auf Basis einer geologisch-geomorphologischen Detailkartierung und GIS-Analyse. Unpublished Diploma Thesis, Institute of Applied Geosciences, University of Graz and Graz University of Technology, in German, 164 pages.

Appendix A

Full papers for all references underlined.
Index running from A1 to A28.

Appendix B

DVD (Digital Versatile Disk) providing videos and computer animations.
See cover page inside in the back.
The content of the DVD can be activated by double-clicking “start.html”.
Further information can be retrieved from “readme.txt”.